Published in final edited form as:

Virology. 2010 October 10; 406(1): 103–116. doi:10.1016/j.virol.2010.07.012.

Characterization of Entry and Infection of Monocytic THP-1 cells by Kaposi's Sarcoma Associated Herpesvirus (KSHV): Role of Heparan Sulfate, DC-SIGN, Integrins and Signaling

Nagaraj Kerur, **Mohanan Valiya Veettil**, **Neelam Sharma-Walia**, **Sathish Sadagopan**, **Virginie Bottero**, **Arun George Paul**, and **Bala Chandran***

H. M. Bligh Cancer Research Laboratories, Department of Microbiology and Immunology, Chicago Medical School, Rosalind Franklin University of Medicine and Science, 3333 Green Bay Road, North Chicago, IL 60064, USA

Abstract

KSHV effectively binds, enters and establishes infection in THP1 cells with initial concurrent expression of latent ORF73 and lytic ORF50 genes and subsequent persistence of ORF 73. KSHV genome persisted for 30 days and lytic cycle could be activated. KSHV utilized heparan sulfate for binding to THP-1 cells and primary monocytes. Blocking DC-SIGN did not inhibit KSHV binding; however, virus entry in THP-1 and in primary monocytes was reduced. In addition to the previously identified integrins α3β1, αvβ3 and αvβ5, integrin α5β1 was also utilized for infection. KSHV entered THP1 cells via clathrin and caveolin mediated endocytosis and did not utilize macropinocytosis as in human dermal endothelial cells, and required an endosomal acidification. Infection also induced phosphorylation of FAK, Src, PI3K, NF-κB and ERK1/2 signaling molecules, and entry was blocked by tyrosine kinase inhibitors. These findings suggest that THP-1 cells are highly useful model for studying KSHV infection of monocytes.

Introduction

Kaposi sarcoma associated herpesvirus (KSHV/HHV8), a γ2-herpesvirus, is etiologically linked with Kaposi Sarcoma (KS) and with two lymphoproliferative disorders, primary effusion lymphoma (PEL) and some forms of multicentric Castleman's disease (MCD). KS is a reactive angioproliferative chronic inflammation associated lesion that is characterized by latently infected spindle cells of endothelial origin, fibroblasts and infiltrating inflammatory cells including monocytes (Ganem, 2006). The microenvironment of KS is rich in several growth factors, chemokines and inflammatory cytokines which are implicated in the pathogenesis of KS (Douglas et al., 2007).

In vivo, KSHV DNA and transcripts have been detected in a variety of cells which include B cells from peripheral blood, B cells of PEL and MCD lesions, flat endothelial cells lining the vascular spaces of KS lesions, typical KS spindle cells, CD45+/CD68+ monocytes in KS lesions, keratinocytes, and epithelial cells (Ganem, 1997; Mocarski, 1997). KSHV DNA is present in a latent form in the vascular endothelial and spindle cells of KS tissues and expression of latency associated LANA-1 (ORF 73), v-cyclin D (ORF 72), v-FLIP (K13)

*Corresponding author. Fax: +1 847 578 3349. bala.chandran@rosalindfranklin.edu.

and Kaposin (K12) genes have been demonstrated in these cells (Dourmishev et al., 2003; Ganem, 1997; Schulz, Sheldon, and Greensill, 2002; Staskus et al., 1997; Zhong et al., 1996). Lytic infection is also detected in KS lesions with <1% of infiltrating inflammatory monocytic cells positive for lytic cycle proteins (Dourmishev et al., 2003; Ganem, 1997).

Detailed analyses of KSHV infection of various in vitro target cells are essential to fully understand the tropism and pathogenesis of KSHV. KSHV infects a variety of target cells in vitro such as human B cells, monocytes, endothelial, epithelial and fibroblast cells as well as several animal cells such as BHK-21 cells, monkey kidney cells, CHO cells, and primary embryonic mouse fibroblast cells (Akula et al., 2001a; Akula et al., 2002; Akula et al., 2001b; Ganem, 1998; Naranatt et al., 2003; Schulz, Sheldon, and Greensill, 2002). However, unlike α and β-herpesviruses, de novo infection of adherent target cells by KSHV does not lead to a productive lytic cycle. Instead, KSHV enters into latency and expresses only a few genes from non-integrated circular episome in the infected cell nucleus. KSHV in vitro infection of human microvascular dermal endothelial cells (HMVEC-d), human foreskin fibroblast cells (HFF), human umblical vein endothelial cells (HUVEC) and human embryonic kidney epithelial cells (293) is characterized by the persistent expression of latent ORF72, ORF73, and K13 genes that is concurrent with the transient expression of a limited number of lytic genes with anti-apoptotic and immune modulation functions, including the lytic cycle switch protein Rta/ORF50, early lytic K8, v-IRF-2, K5, ORF59, ORF8 and late lytic gpK8.1A/B (Krishnan et al., 2004; Lan et al., 2005; Raghu et al., 2009). In HMVEC-d, HFF and 293 cells, expression of latent genes continues while lytic gene expression, except K5, decreases rapidly by 24 h post infection (p.i.) (Bechtel et al., 2003; Krishnan et al., 2004).

KSHV infection involves a complex series of events from binding of target cells to establishment of viral gene expression. These events could be sequentially categorized into six overlapping indiscrete dynamic phases. Phase 1 involves binding to target cells via various receptors overlapping with signal induction (phase 2) followed by virus internalization into host cells (phase 3). In phase 4, viral capsid/tegument traffics through the cytoplasm and in phase 5, viral DNA enters into the nucleus. Phase 6 involves the expression of viral and host genes. Previously, we have extensively characterized the various stages of *de novo* KSHV infection of adherent target cells such as HMVEC-d, HUVEC and HFF cells with a focus on receptors, mode of viral entry, viral gene expression and induction of pre-existing host cell signaling cascade (Akula et al., 2001a; Akula et al., 2002; Akula et al., 2001b; Krishnan et al., 2004; Naranatt, Akula, and Chandran, 2002; Naranatt et al., 2003; Naranatt et al., 2005; Naranatt et al., 2004; Raghu et al., 2007; Raghu et al., 2009; Sharma-Walia et al., 2005; Veettil et al., 2008; Veettil et al., 2006).

KSHV's broad *in vitro* cellular tropism may be in part due to its interactions with the ubiquitous cell surface heparan sulfate (HS) proteoglycan (Akula et al., 2001a; Akula et al., 2001b) which is similar to several other herpesviruses. Our studies demonstrate that α3β1, αVβ3, and αVβ5 integrins play important roles in KSHV infection of adherent target cells, such as HMVEC-d, HFF and 293 cells, including entry and induction of host-signal pathways to facilitate viral infection (Akula et al., 2001a; Akula et al., 2002; Akula et al., 2001b; Naranatt, Akula, and Chandran, 2002; Naranatt et al., 2003; Naranatt et al., 2005; Naranatt et al., 2004; Raghu et al., 2007; Raghu et al., 2009; Sharma-Walia et al., 2005; Veettil et al., 2008; Veettil et al., 2006).

Two studies reported that dendritic cell specific intercellular adhesion molecule-3 (ICAM-3) grabbing non-integrin (DC-SIGN; CD209) plays a role in infection of human myeloid dendritic cells (DCs), macrophages and activated B cells (Rappocciolo et al., 2008; Rappocciolo et al., 2006). KSHV binding and infection were blocked by anti-DC-SIGN monoclonal antibody, mannan (a ligand for DC-SIGN), and by soluble DC-SIGN. However, pretreatment of cells with anti-DC-SIGN antibodies did not completely block KSHV binding and infection. This could be due to binding to HS and integrins which were not tested in these studies.

Though KSHV has been detected in several cells types including spindle cells of endothelial origin, fibroblasts and infiltrating inflammatory cells, KSHV *de novo* infection of targets cells other than HMVEC-d, HUVEC and HFF cells has not been studied in detail. Primary B cells from normal individuals are relatively resistant to in vitro infection with KSHV perhaps due to the lack of HS in these cells (Jarousse, Chandran, and Coscoy, 2008) and infection does not result in immortalization as with γ1-Epstein–Barr virus (EBV). In contrast, activated blood and tonsil B cells were productively infected with KSHV which was shown by the increase in viral DNA, expression of viral lytic and latency proteins, and the production of infectious virus (Rappocciolo et al., 2008). A limited amount of cell death was observed in the infected B-cell cultures compared to that of uninfected cell cultures, suggesting that infectious virus production and subsequent destruction of the cell were restricted to a portion of the activated B cells (Rappocciolo et al., 2008). In contrast, as in endothelial and fibroblast cells, DC and macrophages supported the expression of only a limited number of KSHV lytic genes early after virus entry with little or no production of infectious virus (Rappocciolo et al., 2006).

Monocytic cells represent one of the sites of KSHV infection in KS lesions and are key players in the inflammatory response, a crucial step in the pathogenesis of KS. The monocytic cell line THP-1 has been used as a model cell system to define the potential role of Toll like receptors (TLR) in KSHV infection(West and Damania, 2008). However, infections were carried out by mixing virus with polybrene and by centrifugation (spinoculation) by passing the need for the receptors. Moreover, RNA was isolated at 16 h post-infection (p.i.) for demonstrating TLR and KSHV gene expression. LANA mRNA expression was detected 16 h p.i. and no other viral genes were examined (West and Damania, 2008). Compared to *in vitro* culture of monocytes from human peripheral blood, THP-1 cells are easy to grow. Hence, in order to expand the use of THP-1 cells as a model system for dissecting out KSHV interactions with human monocytes here we systematically examined the various early steps of de novo infection.

Results

KSHV efficiently binds to THP-1 cells

The first essential event in KSHV infection is binding to the target cells. KSHV binding to a variety of cells is mediated through the initial interaction with ubiquitous cell surface HS (Akula et al., 2003; Akula et al., 2001a; Akula et al., 2001b; Wang et al., 2001). We first examined the time kinetics and dose dependence of virus binding to THP-1 cells using ^{3}[H]-thymidine labeled KSHV (Akula et al., 2001a). Dose dependent virus binding was observed in cells incubated with an increasing amount of labeled KSHV (Fig. 1A). The kinetics of binding revealed very efficient KSHV binding with about 80% of maximum binding occurring as early as 5 min p.i. which attained a plateau by 15 min p.i. (Fig. 1B). In both of the above experiments, pretreatment of virus with heparin abrogated the binding by >90% suggesting a very significant role for HS in KSHV binding to THP-1 cells.

Kinetics of KSHV DNA internalization in THP-1 cells

To define KSHV entry, THP-1 cells were infected for 2 h with increasing KSHV DNA copies per cell (5 to 40) and internalized virus copy number was determined by real-time DNA PCR for the ORF73 gene (Krishnan et al., 2004). As expected, KSHV internalization increased with the increasing amount of input virus DNA copy numbers (Fig. 1C). When kinetics of KSHV internalization into THP-1 cells was examined by infecting with 10 KSHV DNA copies per cell for different time periods at 37°C, a significant amount of internalized virus could be detected as early as 30 min p.i., which reached a peak at 90 min p.i., plateaued at 120 min p.i. with a slight decrease at 150 min and 180 min p.i. (Fig.1D). Together, these results demonstrated the efficient entry of KSHV in to THP-1 cells.

Kinetics of nuclear entry of KSHV DNA in THP-1 cells

To determine whether the internalized KSHV reach the infected cell nuclei, THP-1 cells were infected for different time periods at 37°C with 10 KSHV DNA copies per cells, nuclei isolated, and DNA purified from these nuclei were used to determine virus copy number by real-time DNA PCR (Raghu et al., 2007). KSHV genome could be detected in the infected cell nuclei as early as 30 min p.i. which increased rapidly after 60 min p.i. and maximum viral copy numbers were found at 90 and 120 min p.i. (Fig. 2A). These results demonstrated that after entering THP-1 cells, KSHV delivers its DNA into the nucleus, an essential prerequisite for KSHV to establish infection in any target cells.

THP-1 cells support expression of latent ORF73 and lytic ORF50 KSHV genes

KSHV ORF73 encoded LANA-1 plays a role in maintenance of latency and mediates tethering of viral genome to the host chromosome in latently infected cells (Verma, Lan, and Robertson, 2007). KSHV immediate early lytic switch RTA (ORF 50) protein drives the transcription of multiple viral genes involved in lytic replication. Since expression of both these genes play vital roles in the KSHV life cycle, we used real-time RT-PCR to analyze their expression in infected THP-1 cells. As early as 2 h p.i., significant levels of both ORF73 and ORF50 messages were detected (Fig 2B and C). ORF73 messages increased steadily and reached peak by 24 h and sustained levels were observed at 48h p.i. We also observed a robust ORF50 expression at 2 h p.i. that steadily increased reaching a peak at 24-48 h p.i. (Fig 2C). To support the gene expression findings, we examined the expression of LANA-1 protein and late lytic marker envelope glycoprotein gpK8.1A by IFA. A significant number of LANA-1 (26% at 48 h p.i.) and gpK8.1A (30% at 48 h p.i.) positive cells were observed at all time points from 8 h to 48 h p.i. (Fig 3 A and B). These results clearly demonstrated that human monocytic THP-1 cells are susceptible to primary KSHV infection and support concurrent expression of latent and lytic KSHV genes.

KSHV establishes persistent infection in THP-1 cells

KSHV positive PEL derived B cell lines maintain multiple copies of KSHV genome indefinitely. In contrast, endothelial cells derived from KS spindle cells, as well as de novo infected endothelial cells, rapidly loose the KSHV episome (Bechtel et al., 2003). To determine whether the KSHV genome persists in THP-1 cells we examined the presence of viral genome in infected THP-1 cells from 1 through 30 days p.i.

THP-1 cells (1×10^6) infected with 10 KSHV DNA copies per cell for 2 h were washed, trypsinized to remove uninternalized virus and then incubated at 37°C. At different days p.i., DNA was isolated from the cell pellet and KSHV genome copy number persisting in the cells was determined by real-time RT-PCR for the ORF73 gene. Persistent KSHV genome copy number was represented as genome copies per 1×10^6 cells. Since uninfected THP-1 cells divide along with infected cells we reasoned that persistent KSHV genome copy numbers will appear to decrease drastically and hence the estimated viral DNA copy numbers will be probably an under representation of persistence. To overcome this problem and to compensate for the replication of uninfected cells, the copy numbers represented in Fig. 3C were derived by normalizing the copy numbers to total DNA yield from the cell pellet. As seen in endothelial cells (Grundhoff and Ganem, 2004), THP-1 cells also lost

NIH-PA Author Manuscript

NIH-PA Author Manuscript

KSHV genome over time. However, a significant number of KSHV genome copies could be detected after 5 and 30 days p.i. Compared to 1 day p.i., as much as 54% and 34% of KSHV genome copy numbers were detected at 5 and 30 days p.i., respectively (Fig.3C). Taken together, these results suggest that the KSHV genome is maintained in the infected THP-1 cells and genome copy numbers decrease over time.

We next examined whether latent KSHV in THP1 cells can undergo lytic reactivation to produce progeny virus. Infected THP1 cells at 21 days p.i. were left untreated or treated with TPA (20ng/ml). The cell culture supernatants and cells were harvested after 5 days of TPA treatment and KSHV genome copy numbers were determined in by real-time DNA PCR. Compared to uninduced THP1 cells 2.5 and 3-fold increase in KSHV genome copy numbers were observed in TPA induced supernatant and cells, respectively (Fig 3 D and E). Over all, these observations suggested that similar to BCBL1 cells, TPA could induce KSHV lytic reactivation in the infected THP1 cells.

KSHV binding in THP-1 cells involves initial interaction with HS

Like many α, β and γ2 herpesviruses, initial biding of KSHV to adherent target cells involves interaction with HS moieties (Akula et al., 2001a). To determine whether KSHV interaction with THP-1 cells also involves HS molecules, the ability of soluble heparin to inhibit KSHV binding to THP-1 cells was examined. A KSHV binding assay was carried out using heparin pretreated ^{3}[H] thymidine-labeled KSHV as described before (Akula et al., 2001b). KSHV binding was inhibited by more than 80% at heparin concentrations as low as 25ug/ml and similar levels of KSHV binding inhibition was observed even at higher concentrations of heparin pretreatment (Fig. 4A). Furthermore enzymatic removal of cell surface HS with heparinase I and III significantly reduced the KSHV binding by 40-60% (Fig. 4B). However, pre-incubation of KSHV with chondroitin sulfate did not inhibit the KSHV binding suggesting cell surface chondroitin sulfate glycosaminoglycans do not play role in KSHV binding to THP1 cells (Fig. 4B). These results suggest KSHV infection of THP-1 cells involves initial binding interactions with cell surface HS moieties.

DC-SIGN does not play a role in KSHV binding to THP-1 cells

Recent studies by Rappocciolo et al(Rappocciolo et al., 2008; Rappocciolo et al., 2006) suggested a role for DC-SIGN in KSHV binding and entry in human macrophages, dendritic cells and activated B cells. Since THP-1 cells originated from myeloid lineage with about 71% of cells expressing DC-SIGN (Fig. S1) the role of DC-SIGN in KSHV binding was examined. THP-1 cells were pre-incubated with various concentrations of mannan, a ligand for DC-SIGN, and radiolabeled KSHV binding was determined. Mannan did not inhibit KSHV binding significantly, even at concentrations up to 400μg/ml. This suggests an insignificant role for DC-SIGN in KSHV binding to THP-1 cells (Fig. 4C).

Heparan sulfate and DC-SIGN play roles in KSHV entry in THP-1 cells

We next examined whether HS and DC-SIGN play roles in KSHV internalization. HS and DC-SIGN were blocked by heparin and mannan, respectively. As expected from the binding results (Fig.4A), heparin blocked KSHV internalization by more than 80% (Fig.5A). In contrast, KSHV internalization was inhibited by mannan only at very high concentrations (400 and 500ug/ml), and then only to a maximum of about 60% inhibition (Fig.5A). In a parallel experiment where heparin (100μg/ml) and mannan (300μg/ml) were used together to block both HS and DC-SIGN, we did not observe any significant synergetic/additive inhibition (Fig. 5A). Although the inhibition was greater than with mannan alone the values did not vary significantly from the inhibition by heparin alone.

We next examined whether KSHV entry in THP1 cells could be inhibited by blocking with anti-DC-SIGN antibody. As shown the figure 5 B, blocking of DC-SIGN with mouse anti-DC-SIGN mAb inhibited the KSHV internalization by 43%. In contrast, no inhibition was observed in IgG incubated control THP1 cells. Taken together our observations suggest that KSHV uses DC-SIGN as one of the receptor for internalization in THP1 cells.

KSHV-integrin interactions play roles in KSHV infection of THP-1 cells

KSHV utilizes α3β1, αvβ3, αvβ5 integrins for HMVEC-d, HFF and 293 cell infection (Veettil et al., 2008). To determine whether integrins play a role in KSHV infection of THP-1 cells, cells were infected with KSHV which had been pre-incubated with 10μg/ml of commercially available human soluble integrins α3β1, αvβ3, αvβ5, α5β1 and α4β7 at 37° C for 1 h and viral gene expression was examined at 24 h p.i. by real-time RT-PCR. As shown in Fig. 5B, integrins α3β1, αvβ3, αvβ5 and α5β1 inhibited ORF73 expression significantly albeit at varying degrees. Soluble integrin α3β1 exhibited maximal inhibition in ORF73 expression (94%) followed by αvβ5 (83%), α5β1(82%) and αvβ3 (68%). When we used soluble integrin α4β7, that is also present in THP-1 cells as specificity control, we did not observe any inhibition of KSHV gene expression. Heparin pretreatment of virus inhibited gene expression by 90% (Fig 5B). Soluble integrins did not block virus binding (data not shown) and these findings suggest that KSHV interactions with integrins α3β1, αvβ3, αvβ5 and α5β1 are crucial for the post-HS binding stage of establishing infection in THP-1 target cells.

To further demonstrate the physical association between KSHV and the integrins, THP-1 cells infected with KSHV for 1, 5 and 10 min were examined by confocal microscopy for co-localization of virus with integrins. As it can be seen in Fig. 6 A to D, KSHV co-localized with all four integrins. Specificity of these interactions is shown by non-reactivity with αvβ6, an abundant THP-1 cell integrin (Fig.6E). Taken together, these studies suggest that multiple integrins, such as α3β1, αvβ3, αvβ5 and α5β1, play a significant role in KSHV infection of THP-1 cells.

KSHV induces the FAK, Src, PI3K, NF-κB and ERK1/2 signal molecules early during infection of THP-1 cells

Our earlier studies have shown that KSHV, like other viruses, utilizes interactions with multiple integrins and cellular receptors to modulate preexisting signaling cascades to facilitate target cell infection (Graham et al., 2005; Greber, 2002; Marsh and Helenius, 2006; Tufaro, 1997; Veettil et al., 2008). Here we have examined the induction of signaling cascades in KSHV infected THP-1 cells. THP-1 cells were serum starved for 24 h, infected with KSHV (20 DNA copies per cell) and signal induction was examined by western blotting with phospho-specific antibodies.

Focal adhesion kinase (FAK) is a non-receptor tyrosine kinase that resides at the sites of integrin clustering, known as focal adhesions (FA). KSHV infection of THP-1 cells rapidly induced FAK phosphorylation as early as 1 min p.i., and sustained until 15 min p.i. (~1.5 fold) followed by a drop in activation levels (~1.3 fold) to control cells (Fig 7A). HS pretreated KSHV failed to induce FAK phosphorylation demonstrating the specificity of FAK induction and suggested that binding of KSHV to target cells induces FAK activation. Since KSHV infection of THP-1 induced robust FAK activation, we next examined the downstream Src activity upon infection of these cells. As seen in Fig. 7B, KSHV infection induced rapid and robust Src activation of 4.1-fold at 1 min p.i. which was sustained at a higher level even at 30 min p.i.

Phosphatidylinositol 3-kinase (PI3-K) family of heterodimeric lipid kinases control activity and subcellular localization of several signal transduction molecules involved in cell survival, migration, vesicular trafficking and cytoskeletal organization. Compared to uninfected control cells KSHV induced a 2.3, 2.3 and 2.7-fold increase in p85 phosphorylation at 1, 2 and 15 min p.i. respectively, which dropped back to physiological levels at 30 min p.i. (Fig. 7C). As expected, heparin pretreated KSHV did not induce PI-3K phosporylation (Fig.7C).

Nuclear factor kappa B (NF-κB) is a member of the highly conserved Rel family of transcription factors integral to promoting inflammation, cell proliferation and survival. Previously we have shown a sustained induction of NF-κB that plays a critical role in latent and lytic viral gene expression during *de novo* infection of HMVEC-d and HFF cells (Sadagopan et al., 2007). When we examined the infected THP-1 cells for phosphorylated p65, as seen in Fig.7D, KSHV infection induced robust and sustained p65 phosphorylation from 5 min to 4 h p.i.

Extracellular signal-regulated kinase (ERK1/2) is another crucial signaling molecule belonging to the mitogen-activated protein kinase (MAPK) super family that can mediate cell proliferation and apoptosis. Previously we have observed that ERK1/2 induced early during KSHV infection is critical for initiating viral gene expression as well as for modulating host genes in HMVEC-d and HFF cells (Sharma-Walia et al., 2005). Here, we observed about 2.4-fold ERK1/2 activation as early as 5 min p.i. of THP-1 cells with a peak at 15 min p.i. (3.2 fold) (Fig. 7E). Taken together, our data demonstrate that KSHV induces a robust FAK, Src and PI3K response early during *de novo* infection and sustained NF- κB and ERK1/2 induction during the observed 4 h p.i.

Tyrosine kinases play roles in KSHV infection of THP-1 cells

Genistein and tyrphostin are potent inhibitors of protein tyrosine kinases (PTK) and can block variety cellular signaling events involving tyrosine phosphorylation. To determine the effect of blocking signal induction on KSHV infection, THP-1 cells were pre-incubated with genistein and tyrphostin for 1 h, washed and infected with 10 KSHV DNA copies/cell for 2 h and internalized KSHV viral DNA was quantified by real-time DNA PCR for the ORF73 gene (Krishnan et al., 2004). Both tyrphostin and genistein inhibited KSHV internalization by 40% and 70%, respectively (Fig. 7F). This suggested that cellular kinase signaling events play critical roles in KSHV entry into THP-1 cells.

KSHV entry into THP-1 cells involves clathrin and caveolin mediated endocytic pathways

To examine the mode of KSHV entry, THP-1 cells pretreated with non-toxic concentrations of various endocytosis inhibitors were infected with KSHV (10 DNA copies/cell) for 2 h and internalized viral DNA was quantitated. Chlorpromazine, a clathrin mediated endocytosis inhibitor and filipin a caveolar pathway inhibitor, blocked KSHV entry into THP-1 by 51% and 45%, respectively (Fig. 8A). Cytochalasin D, a cell permeable mycotoxin, inhibits macropinocytosis by blocking the formation of microfilaments and microtubules. EIPA, a potent inhibitor of Na+/H+ exchangers, is also known to inhibit marcopinocytosis. When THP-1 cells were pre-incubated with the Cytochalasin D and EIPA, no significant effect on KSHV entry was observed (Fig. 8A). In a parallel experiment where chlorpromazine (1.5μg/ml) and filipin (2.5μg/ml) were used together to block both clathrin and caveolar endocytic pathways, we observed a significantly higher inhibition (72.3%) in KSHV internalization compared entry inhibition by chlorpromazine (51%) or filipin (45%) alone (Fig. 8A). These results suggested that KSHV utilizes both clathrin and caveolin mediated endocytic pathways for entry into THP-1 cells while macropinocytosis does not appear to play a role in THP-1 infection.

NH_4Cl is a weak lysomotropic base known to inhibit endosomal acidification and bafilomycin A1 a specific and potent inhibitor of vacuolar H^+ ATPase inhibits endosomal and lysosome acidification. Preincubation of THP-1 cells with non-cytotoxic concentration of NH_4Cl (100mM) and bafilomycin A1 (50nM) results in decreased ORF73 gene expression by 45% and 67% respectively, suggesting a requirement for low pH endocytic environment in the infectious process of THP-1 cells (Fig. 8B).

KSHV infection of primary monocytes involves role of heparan sulfate and DC-SIGN

Though THP1 cells are monocytic cell line, these cells might significantly differ from primary monocytes in some characteristics. Therefore, we next examined whether KSHV infection of THP1 cells resembles the infection in primary monocytes. We found that soluble heparin and heparinase treatment of primary monocytes inhibit the KSHV binding by 60-80% and 40-53% respectively. In contrast, soluble chondroitin sulafte did not have any effect on KSHV binding. Furthermore, blocking DC-SIGN with anti-DC-SIGN mAb inhibited KSHV internalization by 60 %. Over all these observations suggest that, similar to THP1 cells, heparan sulfate play roles in KSHV binding to primary monocytes and DC-SIGN also play roles in KSHV entry in primary monocytes.

Discussion

Depending upon the target cell type, virus infectious pathways can vary greatly in several aspects such as the choice of receptor, mode of internalization and nature of virus life cycle. Our current study uncovers several aspects associated with KSHV infection of monocytes: (a) We demonstrate the role of HS in monocyte infection; (b) This is first study showing KSHV persistence in infected THP1 for periods as long as 30 days pi.; (c) Our study demonstrates that KSHV's mode of internalization in monocytic cells differs from HMVEC-d cells in that the virus utilizes clathrin and caveolin mediated endocytosis and not macropinocytosis, and (d) endocytosis is followed by the requirement of low intracellular pH for infection. When one compares the present study with what is known about KSHV infection in other target cells, such as adherent HMVEC-d, HUVEC, HFF and dendritic cells and suspension cells including primary activated human B cells and monocytes, several similarities and differences emerge which are summarized and discussed here.

KSHV readily binds THP-1 cells with comparable efficiency and agree with previous studies (Akula et al., 2001b; Dezube et al., 2002; Raghu et al., 2007) that demonstrated efficient binding of labeled KSHV to a variety of target cells including primary monocytes, endothelial, epithelial and fibroblast cells. The entry kinetics and nuclear delivery of viral DNA in THP-1 cells were similar to our earlier findings in adherent HMVEC-d, HFF and HUVEC cells (Krishnan et al., 2004; Raghu et al., 2007; Raghu et al., 2009).

Our previous studies in HMVEC-d and HUVEC cells showed the sustained expression of KSHV latent transcripts and high levels of lytic switch ORF50 at 2 h p.i. which subsequently declined (Krishnan et al., 2004; Raghu et al., 2009). Rappocciolo et al., utilized peripheral blood $CD14^+$ monocytes to generate mature dendritic cells by incubating with CD40L (Rappocciolo et al., 2006). Macrophages were generated by incubating $CD14^+$ monocytes with 5% heat inactivated, pooled human AB^+ serum, and 1000 U/ml recombinant human GM-CSF for7 days, and treated overnight with 20 ng/ml human IL-13 (Rappocciolo et al., 2006). KSHV infection of DCs and macrophages was similar to the infection of HMVEC-d and HFF cells. They observed the expression of latent ORF 73 as well as lytic ORF59 and gpK8.1A during 48 h p.i. with a subsequent nonproductive, latent viral infection without significant viral DNA replication (Rappocciolo et al., 2006).

Our studies also demonstrate that THP-1 cells are susceptible to primary KSHV infection and support concurrent expression of latent and lytic KSHV genes. Despite sustained high levels of ORF50 expression, we did not observe any sign of KSHV progeny production as there was no increase in KSHV DNA in infected THP-1 cells. Thus, as in monocyte derived dendritic cell, KSHV infection of THP-1 cells is also characterized by a latent viral infection without significant viral DNA replication. However, we also extended the studies by Rappocciolo et al., and demonstrate that the KSHV genome persisted in THP-1 cells for the observed 30 days p.i and that the latent KSHV in THP1 could be induced with TPA to undergo lytic reactivation to produce viral progeny. However the number of KSHV genomes detected in TPA induced cells and cell culture supernatants were less than 150 and 80/100ng of DNA respectively. This low genome copy number is possibly due to relatively lesser number of infected cells at 21 days p.i.

Though the genome copy numbers decreased over time, sustainability of an appreciable amount of KSHV genome up to 30 days suggests that THP-1 cells could also be used as a model system for examining the latency program and host factors involved in the establishment and maintenance of latency. Further studies are essential to determine how long KSHV infection persists in THP-1 cells, nature of the genome and whether the lytic cycle can be induced from these cells either spontaneously or by chemicals.

Our studies show that KSHV interacts with HS and multiple integrins for THP-1 cell infection. The importance of HS in KSHV infection is also shown by Jarousse et al., who demonstrated that the low abundance of surface HS is one of the contributing factors for the reduced susceptibility of B cell lines to the KSHV infection (Jarousse, Chandran, and Coscoy, 2008). The previous studies in monocytes by Rappocciolo *et al* predominantly examined the role of DC-SIGN in KSHV binding and entry. Role of HS in KSHV infection of monocytes has not been explored before. We demonstrated here that KSHV utilizes HS in THP-1 cells and in primary monocytes as a primary binding receptor to increase the efficiency of infection. This is similar to the use of HS in other target cells such as HMVEC-d, HFF, HEK-293 and B-cells (Akula et al., 2003; Akula et al., 2001a; Akula et al., 2001b; Wang et al., 2001). HS has been shown to be involved in initial interaction with target cells by several viruses including herpes simplex virus type 1 and 2 (HSV-1 and HSV-2), cytomegalovirus (CMV), HIV-1 and human papillomavirus (HPV) (Compton, Nowlin, and Cooper, 1993; Giroglou et al., 2001; Tyagi et al., 2001; WuDunn and Spear, 1989).

DC-SIGN has been shown to play a significant role in KSHV binding to human peripheral blood $CD14^+$ monocyte derived dendritic cells and macrophages (Rappocciolo et al., 2006). However, in THP-1 cells blocking DC-SIGN with mannan had no effect on KSHV binding, and blocking DC-SIGN with mannan and anti-DC-SIGN antibodies inhibited KSHV DNA internalization. Furthermore, entry inhibition by mannan was only observed at very high mannan concentrations. This suggests that DC-SIGN may be playing a role in the post-binding entry stage of THP-1 cell infection as well as in primary monocytes. We were not able to observe the role of DC-SIGN at the stage of virus binding probably due to highly abundant HS masking the effect of DC-SIGN. It is well known that virus binding and entry are very distinct processes involving different receptors. Binding of viruses can occur at 4°C and entry is an energy dependent phenomenon (blocked by sodium azide). Viruses can bind to target cells to specific receptors and may not enter if the secondary receptors are absent. Initial interaction with the binding receptor is believed to results in conformation changes that are required to interact with additional receptors. We believe that KSHV binding to HS is essential for subsequent interactions with integrins (as shown by us in HMVEC-d cells; Veettil et al., 2008) and DC-SIGN in THP-1 cells. Hence, virus still binds to HS even in the presence of mannan. However, prevention of subsequent interaction with DC-SIGN by mannan treatment probably blocks DC-SIGN interactions that plays role in entry.

Our earlier studies have shown that α3β1, αvβ3 and αvβ5 integrins play a role in the post-HS binding stage of KSHV infection of HMVEC-d, HFF, 293 and Vero cells (Akula et al., 2002; Veettil et al., 2008). Interestingly, KSHV in addition to using the previously identified α3β1, αvβ3 and αvβ5 integrins also uses α5β1 integrins for infection of THP-1 cells. The identity of KSHV envelope glycoproteins involved in receptor interactions and the role of xCT/CD98 for THP-1 infection needs to be investigated further.

Herpesviruses and other enveloped viruses enter their target cells *in vitro* either by endocytosis or by fusion of their envelope with the plasma membrane or with the endosomal membrane following internalization by endocytosis (Hutt-Fletcher, 2007; Nicola, McEvoy, and Straus, 2003; Nicola and Straus, 2004; Sinzger, 2008). For example, entry of HSV-1 into Vero and HEp-2 cells is known to occur via fusion at the plasma membrane (Fuller, Santos, and Spear, 1989; Fuller and Spear, 1987). Whereas CHO-K1 and HeLa cells support a pH-dependent endocytic route of entry, suggesting HSV enters target cells by more than one pathway in a cell-specific manner (Nicola, McEvoy, and Straus, 2003). Similarly EBV enters primary B cells via endocytosis and human epithelial cells via fusion at the plasma membrane (Hutt-Fletcher, 2007).

Multiple endocytic pathways operate concurrently at the cell surface, differing in their mechanism of formation, molecular machinery involved and cargo destination. The clathrin coated pit pathway is used for entry by many viruses such as HSV, HIV-1, influenza virus, adenovirus and poliovirus (Kalia and Jameel, 2009), while the caveolar pathway is the main mode of entry for simian virus 40, polyoma virus and echovirus (Anderson, Chen, and Norkin, 1996; Gilbert and Benjamin, 2000; Mackay and Consigli, 1976; Pietiainen et al., 2004; Stang, Kartenbeck, and Parton, 1997). However, many viruses are also able to utilize clathrin and caveolin independent pathways, which are less understood in terms of cargo specificity and molecular machineries involved. For example, several members of the vaccinia, adeno and picorna families have been reported to use macropinocytosis, an endocytic dynamin independent mechanism normally involved in fluid uptake (Amstutz et al., 2008; Mercer and Helenius, 2008; Mercer and Helenius, 2009).

Use of multiple endocytic pathways and receptors for infection of target cells has been frequently observed in several viruses, while the use of one pathway might predominate over another depending upon the target cell type. Influenza virus enters cells predominantly via clathrin-mediated endocytosis, however the existence of non-clathrin dependent and non-caveolar dependent endocytic pathways has also been demonstrated (Sieczkarski and Whittaker, 2002). Similarly, KSHV utilizes endocytosis as mode of entry to infect HFF, BJAB, HEK 293 and activated primary B cells (Akula et al., 2003; Akula et al., 2001b; Rappocciolo et al., 2008). However, for infectious entry into endothelial cells (HMVEC-d and HUVEC), KSHV utilizes an actin polymerization dependent macropinocytic pathway (Raghu et al., 2009). In contrast to endothelial cell infection, our observations suggest that KSHV does not enter THP-1 cells by macropinocytosis. However, the reduction in KSHV internalization in chlorpromazine and filipin pretreated THP-1 cells by 51% and 45% clearly demonstrates that KSHV entry in these cells involves clathrin and caveolin dependent endocytic pathways. In addition, when chlorpromazine and filipin were used in combination much higher KSHV entry inhibition (72.3%) was observed suggesting concurrent usage of both the pathways by KSHV. Supporting this finding, KSHV has been shown to induce the TLR3 pathway in THP-1 cells (West and Damania, 2008). Since TLR3 is sequestered in the endosome and our finding explains the possibility that KSHV is being exposed to TLR3 in the endosome early during the infection. Macropinocytosis appears to play no role in infection and other modes of entry such as fusion of viral envelope at the cell membrane cannot be ruled out at the present time.

After endocytic internalization, virus particles are sequestered in the endosome until proper conditions are met for release of the viral genome. For many enveloped viruses a low pH in the sorting/late endosome is the trigger for conformational changes necessary to initiate membrane fusion events leading to release of the viral genome at its site of replication. However several other viruses penetrate the cytosol in a pH independent manner. For example, EBV and duck hepatitis B virus enter certain types of cells by endocytosis without a requirement for a low pH to penetrate the cytosol (Kock, Borst, and Schlicht, 1996; Miller and Hutt-Fletcher, 1992). KSHV infection in HFF, HEK 293, HMVEC-d and HUVEC cells is inhibited by preventing endosomal acidification with bafilomycin A or NH_4Cl (Akula et al., 2003; Raghu et al., 2009). In agreement with previous studies in other target cells, our observations in THP-1 show that NH_4Cl and bafilomycin A1 block KSHV gene expression, suggesting a requirement for a low pH intracellular environment for KSHV infection. However, the incomplete inhibition of KSHV gene expression also hints at a possibility of coexistence of pH independent entry portals in THP-1 cells.

Viruses and many other pathogens are known to exploit ligand mimicry by which they subvert host signaling molecules for their benefit (Stewart and Nemerow, 2007; Triantafilou, Takada, and Triantafilou, 2001). KSHV interactions with multiple integrins and associated protein complexes such as xCT/CD98 in HMVEC-d cells triggers induction of pre-existing integrin-associated host cell signal pathways, such as FAK, Src, PI3-K, protein kinase C, Rho-GTPases, MEK, ERK1/2, and NF-κB which are essential for the internalization of viral particles, modulation of actin cytoskeleton and microtubule polymerization required for cytoplasmic trafficking of viral particles, nuclear delivery of viral DNA, and initiation of viral-gene expression (Akula et al., 2002; Naranatt et al., 2003; Naranatt et al., 2005; Raghu et al., 2007; Sadagopan et al., 2007; Sharma-Walia et al., 2005; Veettil et al., 2006). Similar to the adherent HMVEC-d and HFF cells, KSHV induces host cell FAK, Src, PI-3K, ERK1-2 and NF-kB in THP-1 cells. Inhibition of KSHV entry by tyrosine kinase inhibitors demonstrates that KSHV infection of THP-1 cells require various signaling cascades to facilitate its entry and establishment of infection.

Though THP1 cells are derived from monocytic cells, it is conceivable that these cells would differ from primary monocytes in several aspects. However our studies here show that THP1 cell infection resembles infection of primary monocytes in the aspects studied here. We found that similar to THP1 cells heparan sulfate and DC-SIGN play significant roles in KSHV infection of primary monocytes. Since THP-1 cells can be grown easily compared to primary monocytes from human peripheral blood, the characterization of infection described here demonstrates that THP-1 cells can be exploited as a good model to study KSHV infection of monocytes, particularly the mode of infection, receptors, role of host cell signals in infection, cytokine induction, latency and host factors involved in the establishment and maintenance of latency.

Materials and Methods

Cell lines and viruses

THP-1 cells from the American Type Culture Collection (Manassas, VA) and KSHV carrying BCBL-1 cells grown in RPMI 1640 medium (Gibco BRL, Grand Island, NY) containing 10% fetal calf serum (HyClone, Logan, UT), 25 mM HEPES and antibiotics were maintained at 37°C in 5% CO_2 atmosphere. Purified KSHV preparations used in the study were produced by inducing KSHV lytic cycle from BCBL1-1 cells as described previously (Krishnan et al., 2004; Naranatt, Akula, and Chandran, 2002; Naranatt et al., 2003; Naranatt et al., 2005; Naranatt et al., 2004; Raghu et al., 2007; Sharma-Walia et al., 2005). Briefly, KSHV lytic cycle was induced in BCBL-1 cells by treatment with TPA (20 ng/ml) for 5 days. The cells were then centrifuged, and the supernatant was collected. The supernatants were centrifuged at 14,000 rpm for 2 h at 4° C to pellet the virus. The viral pellets were resuspended, centrifuged at low speed several times to remove cell debris and filtered through 0.45μ. The resulting supernatant was then centrifuged at 30,000 rpm, for 2 h at 4° C. The viral pellet was resuspended in serum free DMEM. KSHV DNA was extracted from the virus, and copy numbers were quantitated by real-time DNA PCR using primers amplifying the KSHV ORF73 gene as described previously (Krishnan et al., 2004; Naranatt et al., 2005; Raghu et al., 2007; Sharma-Walia et al., 2005; Veettil et al., 2008). Radiolabeled KSHV was prepared as described previously (Akula et al., 2001a; Akula et al., 2002; Akula et al., 2001b)

Blood donors

Blood from healthy donors was used in this study for purifying $CD14^+$ monocytes. Informed consent was obtained according to Rosalind Franklin University Institutional Review Board guidelines.

Preparation of primary monocytes from blood

The peripheral blood mononuclear cell (PBMC) fractions were collected from the heparinized blood by differential density centrifugation over Ficoll-Paque PLUS (GE Healthcare, Piscataway, NJ). After washing cells twice in hank's balanced salt solution, monocytes were purified from the PBMC via magnetic separation using beads coated with anti-CD14 antibody following the manufacturer's instructions (Miltenyi Biotec, Germany). The purity of the fractionated primary monocytes, as determined by flow cytometric analysis with FITC conjugated anti-CD14 antibody, was >95%. Purified $CD14^+$ monocytes were used immediately for the KSHV binding and entry studies.

Antibodies and reagents

Heparin, chondroitin sulfate, mannan, chlorpromazine, cytochalasin D, EIPA (5-N-ethyl-N-isoproamiloride), filipin, NH_4Cl, Genistien, Tyrphostin 1 (protein tyrosine kinase inhibitors), heparinase I, heparinase III were obtained from Sigma, St Louis, MO. Paraformaldehyde was from Electron Microscopy Sciences, Hatfield, PA. Mouse anti-DC-SIGN mAb (clone 120507) was from R&D Systems, Minneapolis, MN. FITC conjugated anti-CD14 antibody was from (eBioscience, San Diego, CA.), Mouse anti-pY397 FAK, mouse anti-total FAK and anti-total PI3K antibodies were obtained from BD Biosciences, San Jose, CA. Anti-phospho-Src (PY418), anti-total Src and anti-phosphotyrosine (PY20) antibodies were obtained from Upstate Biotechnology, Lake Placid, N.Y. Rabbit antibodies detecting the phosphorylated forms of ERK1/2 (Thr 202/Tyr 204 phospho-p44/42 mitogen-activated protein kinase [MAPK]), mouse anti phospho-p65 and total p65, were obtained from Cell Signaling Technology, Beverly, MA. Total ERK2 antibody was from Santa Cruz Biotechnology Inc., Santa Cruz, CA. Mouse monoclonal anti-KSHV gpK8.1A antibodies (4A4) have been described before (Zhu, Puri, and Chandran, 1999). Rat monoclonal anti-LANA-1 antibody was obtained from Advanced Biotechnologies Inc., Columbia, MD. Anti-rabbit and anti-mouse horseradish peroxidase linked antibodies were from Kirkegaard and Perry Laboratories, Inc., Gaithersberg, MD. Secondary antibodies for immunofluorescence were purchased from Molecular Probes-Invitrogen Corp., Carlsbad, CA. Rabbit anti-integrin α3 and β1 and soluble human integrins α3β1, αvβ3, αvβ5 and α5β1 were from Upstate Biotechnology, Lake Placid, N.Y. Recombinant human integrin α4β7 was from R&D systems, Minneapolis, MN.

Radiolabeled-KSHV binding assay

1×10^6 THP-1 cells were washed and mildly fixed with 0.1% paraformaldehyde. The fixed cells were further washed twice with RPMI containing 5% FBS and incubated with [^{3}H] labeled KSHV for 1 h at 4°C. After incubation, the cells were washed five times and lysed and the radioactive virus was precipitated with trichloroacetic acid and counted in a scintillation counter (Akula et al., 2001a; Akula et al., 2002; Akula et al., 2001b).

Heparinase treatment

For enzymatic removal of cell surface heparan sulfate, THP1 cells and primary monocytes were incubated with serum free DMEM containing heparinase I and III (5 and 10 units/ml) or DMEM alone for 2 h at 37 °C. The untreated and treated cells were washed and used for the KSHV binding studies as described below.

Virus binding assay using non-radioactive/unlabeled KSHV

Untreated or heparinase I and III treated THP-1 cells/primary monocytes were washed and mildly fixed with 0.1% paraformaldehyde. The fixed cells were further washed twice with RPMI containing 5% FBS and incubated with KSHV for 1 h at 4°C. After incubation, unbound KSHV were removed by washing and DNA was isolated from the cells. Cell bound KSHV were quantitated by real-time DNA PCR for ORF73 as described previously (Naranatt et al., 2005; Raghu et al., 2007).

Cytotoxicity assays

THP-1 cells were incubated with RPMI 1640 medium containing different concentrations of various inhibitors and cellular toxicity by using an MTT assay kit (ATCC) in accordance with the manufacturer's recommendations.

Preparation of DNA and RNA

Isolation of total DNA from the viral stocks and infected or uninfected THP-1 cells by a DNeasy tissue kit (QIAGEN, Inc., Valencia, CA) and isolation of total RNA from infected or uninfected cells using an RNeasy kit (QIAGEN) were carried out as described previously (Krishnan et al., 2004; Krishnan et al., 2005; Raghu et al., 2007).

Measurement of KSHV DNA internalization and nuclear delivery

THP-1 cells were infected with 10 DNA copies per cell of KSHV for different time points or for 2 hrs with 10 to 40 DNA copies per cell. After incubation with virus, cells were washed twice with PBS to remove unbound virus. Cells were treated with 0.25% trypsin-EDTA for 5 min at 37°C to remove the bound, non-internalized virus and washed twice more to remove the virus and trypsin-EDTA. Total DNA isolated from cells or from nuclear fractions was tested by real-time DNA PCR for ORF73 as described previously (Naranatt et al., 2005; Raghu et al., 2007). For examining the role of DC-SIGN in KSHV internalization, THP-1 cells and were pre-incubated with different concentrations of mannan, infected with 10 DNA copies per cell and KSHV DNA internalization was examined as described above. To examine KSHV internalization after blocking DC-SIGN, THP1 cells and primary monocytes were pre-incubated with mouse anti-DC-SIGN mAb or mouse IgG (15μg/ml) for 1 h at 4° C. The antibody pre-incubated cells were then incubated with KSHV (10 genome copies/cell) at 4° C for 1h followed by at 37° C for 1 h and KSHV DNA internalization was examined as described above. To examine the role of heparan sulfate in KSHV internalization, KSHV pre-incubated with different concentrations of heparin (25μg, 50μg, 100μg and 150μg/ml) for 1 h at 37° C were incubated with THP-1 for 2 hrs and KSHV DNA internalization was determined as described above.

For determining the role of signal induction in KSHV entry, THP-1 cells were preincubated with Tyrphostin I (50μM and 100μM) and Genistein (50μM and 100μM) for 1 h at 37°C. Untreated and treated cells were infected with KSHV (10 DNA copies/cell) for 2 hrs and

NIH-PA Author Manuscript

NIH-PA Author Manuscript

internalized KSHV copies were determined by real-time DNA PCR as described above. To determine the mode of KSHV entry, THP-1 cells were pre-incubated (1 h at 37°C) with chlorpromazine (1.5μg/ml), filipin (2.5μg/ml), EIPA (1.5μg/ml), cytochelasin D (2.5μg/ml) as well as with combination of chlorpromazine (1.5μg/ml) and filipin (2.5μg/ml) and infected with KSHV (10 DNA copies/cell) and KSHV internalization was determined as described above.

Examination of KSHV gene expression by real-time reverse transcription (RT)-PCR

1×10^6 THP-1 cells infected with 30 DNA copies per cell of KSHV for different time points (2 h, 8 h, 24 and 48 h p.i), were washed three times with 1× PBS to remove the unbound virus and lysed with RLT buffer (QIAGEN). Total RNA was isolated from the lysate using RNeasy kits (QIAGEN) according to the manufacturer's protocols and quantified spectrophotometrically. The abundance of ORF 50 and ORF 73 transcripts was detected by real-time rRT-PCR using specific real-time primers and TaqMan probes as described previously (Krishnan et al., 2004; Sharma-Walia et al., 2005). The expression levels of the viral transcripts were normalized to 18s rRNA gene expression. Possibility of false signal from trace amounts of viral DNA were ruled out by including control reactions with RNase treated samples and reactions without rT*th* DNA polymerase enzyme.

For examining the role of integrins in establishment of KSHV gene expression, THP-1 cells were infected with 30 DNA copies per cell of KSHV that were pretreated with 10μg/ml of human soluble integrins (α3β1, αvβ3, αvβ5, α5β1 and α4β7) and expression of ORF73 was determined at 24 h p.i. as described above. For examining the requirement of endosomal acidification for KSHV infection, THP-1 cells were pre-incubated with 100mM NH_4Cl for 3 h or 50nM bafilomycin A for 1h, followed by incubation with KSHV (30 DNA copies/cell) for 2 h. Untreated and treated cells were washed, trypsinized to remove uninternalized KSHV and then ORF73 gene expression was examined at 24 h p.i.

KSHV DNA nuclear delivery assay

THP-1 cells infected with KSHV were collected at different time points, washed, and treated with trypsin-EDTA (0.25% trypsin and 5 mM EDTA) to remove uninternalized virus. Nuclear fractions were prepared from infected and uninfected THP-1 cells using a Nuclei EZ isolation kit (Sigma) following the manufacturer's recommendations. The purity of nuclear preparations was assessed by immunoblotting using anti-lamin B and anti-tubulin antibodies. DNA isolated from infected cell nuclei were used for determining the nuclear delivery of KSHV genome by real-time DNA PCR as described previously (Naranatt et al., 2005; Raghu et al., 2007).

Immunofluorescence assay (IFA)

THP-1 cells were infected with 30 DNA copes per cell of KSHV for 2 h. Mock infected and infected cells were washed, treated with 0.5% trypsin to remove uninternalized KSHV, and incubated in complete growth media for different time points (8 h, 24 h and 48h p.i.). Cells were washed, fixed with 2% paraformaldehyde on a glass slide, permeabilized with 0.2% Triton X-100, blocked with Image-iT™ FX signal enhancer (Invitrogen) for 20 min and then incubated with rat anti-KSHV ORF73 (1:100) and mouse anti-gpK8.1 antibodies. Cells were washed with PBS, incubated with anti-rat Alexa Fluor 488 antibodies (1:1000) and anti-mouse Alexa Fluor 594 antibodies (1:2000), respectively, for 1 h at RT. The cells were washed, mounted with antifade reagent containing DAPI (4′,6′-diamidino-2-phenylindole) and visualized under a Nikon fluorescent eclipse 80i microscope. Images were processed using Metamorph imaging software. DC-SIGN staining in uninfected THP1 cells was done as described above using mouse anti-DC-SIGN mAb and goat ant-mouse Alexa Flour 488 secondary antibody.

Laser-scanning confocal immunofluorescence

THP-1 cells infected with 10 DNA copies per cell of KSHV were fixed for 10 min with 2% paraformaldehyde, permeabilized with 0.2% Triton X-100 for 5 min, washed and blocked with Image-iT™ FX signal enhancer (Invitrogen) for 20 min. Mock and KSHV infected cells were incubated with rabbit anti-KSHV gB antibody or mouse anti-integrin antibodies followed by goat anti-rabbit Alexa Fluor 488 and goat anti-mouse Alexa Fluor 594-labeled antibody. The Olympus Fluoview 300 fluorescence confocal microscope was used for imaging and analysis was performed using Fluoview software (Olympus, Melville, NY).

Western blot analysis

Infected and uninfected cells were lysed in RIPA lysis buffer containing a protease inhibitor cocktail. Cellular debris was removed by centrifugation at 13,000 × g for 20 min at 4°C. The protein concentration of the clarified supernatant was determined with a micro-bicinchoninic acid protein assay kit (Pierce, Rockford, IL). Each sample was heated at 95°C for 5 min, resolved by 10% SDS-PAGE, and transferred to a nitrocellulose membrane. Phosphorylated FAK, Src, NF- κB and ERK1/2 were assessed by immunoblotting with specific antibodies. To confirm equal protein loading, membranes were stripped and reprobed with anti-total FAK, Src, NF- κB and ERK1/2 antibodies. Horseradish peroxidase-conjugated secondary antibodies were used for detection. Immunoreactive bands were developed by enhanced chemiluminescence reaction (NEN Life Sciences Products, Boston, MA) and quantified by following standard protocols (Sharma-Walia et al., 2004). To examine phosphorylated PI3K, THP-1cells infected with KSHV (20 DNA copies/cells) for different times at 37°C were washed, lysed in RIPA lysis buffer, clarified by centrifugation for 15 min at 4°C and normalized to equal amounts of total protein. The lysate was incubated for 2 h with anti-total PI3K antibody at 4°C, and immune complexes were captured using 10 μl of protein G-Sepharose. They were washed three times with RIPA lysis buffer, boiled with SDS-PAGE sample buffer, and run on a 10% SDS-PAGE gel. The phosphorylated PI3K was detected by immunoblotting with mouse anti-phosphotyrosine (PY20) antibody. To confirm equal protein loading, membranes were stripped and reprobed with anti-total PI3K antibodies.

Flow cytometry

THP1 cells for fluorescence-activated cell sorting (FACS) analysis were prepared following manufacturer's guidelines (BD Biosciences). DC-SIGN staining was performed using anti-DC-SIGN mAb. The data were collected using FACSCalibur flow cytometer (Becton Dickinson) and analyzed with CellQuest Pro software (Becton Dickinson) at the Rosalind Franklin University of Medicine and Science flow cytometry core facility.

Supplementary Material

Refer to Web version on PubMed Central for supplementary material.

Acknowledgments

This study was supported in part by Public Health Service grant AI 057349 and the RFUMS H. M. Bligh Cancer Research Fund to B.C. We thank Keith Philibert for critically reading the manuscript. We thank Rita Levine and Robert Dickinson for the help in FACS analyses at the RFUMS FACS/Cell sorter core facility.

References

Akula SM, Naranatt PP, Walia NS, Wang FZ, Fegley B, Chandran B. Kaposi's sarcoma-associated herpesvirus (human herpesvirus 8) infection of human fibroblast cells occurs through endocytosis. J Virol. 2003; 77(14):7978–90. [PubMed: 12829837]

Akula SM, Pramod NP, Wang FZ, Chandran B. Human herpesvirus 8 envelope-associated glycoprotein B interacts with heparan sulfate-like moieties. Virology. 2001a; 284(2):235–49. [PubMed: 11384223]

Akula SM, Pramod NP, Wang FZ, Chandran B. Integrin alpha3beta1 (CD 49c/29) is a cellular receptor for Kaposi's sarcoma-associated herpesvirus (KSHV/HHV-8) entry into the target cells. Cell. 2002; 108(3):407–19. [PubMed: 11853674]

Akula SM, Wang FZ, Vieira J, Chandran B. Human herpesvirus 8 interaction with target cells involves heparan sulfate. Virology. 2001b; 282(2):245–55. [PubMed: 11289807]

Amstutz B, Gastaldelli M, Kalin S, Imelli N, Boucke K, Wandeler E, Mercer J, Hemmi S, Greber UF. Subversion of CtBP1-controlled macropinocytosis by human adenovirus serotype 3. Embo J. 2008; 27(7):956–69. [PubMed: 18323776]

Anderson HA, Chen Y, Norkin LC. Bound simian virus 40 translocates to caveolin-enriched membrane domains, and its entry is inhibited by drugs that selectively disrupt caveolae. Mol Biol Cell. 1996; 7(11):1825–34. [PubMed: 8930903]

Bechtel JT, Liang Y, Hvidding J, Ganem D. Host range of Kaposi's sarcoma-associated herpesvirus in cultured cells. J Virol. 2003; 77(11):6474–81. [PubMed: 12743304]

Compton T, Nowlin DM, Cooper NR. Initiation of human cytomegalovirus infection requires initial interaction with cell surface heparan sulfate. Virology. 1993; 193(2):834–41. [PubMed: 8384757]

Dezube BJ, Zambela M, Sage DR, Wang JF, Fingeroth JD. Characterization of Kaposi sarcoma-associated herpesvirus/human herpesvirus-8 infection of human vascular endothelial cells: early events. Blood. 2002; 100(3):888–96. [PubMed: 12130499]

Douglas JL, Gustin JK, Dezube B, Pantanowitz JL, Moses AV. Kaposi's sarcoma: a model of both malignancy and chronic inflammation. Panminerva Med. 2007; 49(3):119–38. [PubMed: 17912148]

Dourmishev LA, Dourmishev AL, Palmeri D, Schwartz RA, Lukac DM. Molecular genetics of Kaposi's sarcoma-associated herpesvirus (human herpesvirus-8) epidemiology and pathogenesis. Microbiol Mol Biol Rev. 2003; 67(2):175–212. table of contents. [PubMed: 12794189]

Fuller AO, Santos RE, Spear PG. Neutralizing antibodies specific for glycoprotein H of herpes simplex virus permit viral attachment to cells but prevent penetration. J Virol. 1989; 63(8):3435–43. [PubMed: 2545914]

Fuller AO, Spear PG. Anti-glycoprotein D antibodies that permit adsorption but block infection by herpes simplex virus 1 prevent virion-cell fusion at the cell surface. Proc Natl Acad Sci U S A. 1987; 84(15):5454–8. [PubMed: 3037552]

Ganem D. KSHV and Kaposi's sarcoma: the end of the beginning? Cell. 1997; 91(2):157–60. [PubMed: 9346233]

Ganem D. Human herpesvirus 8 and its role in the genesis of Kaposi's sarcoma. Curr Clin Top Infect Dis. 1998; 18:237–51. [PubMed: 9779358]

Ganem D. KSHV infection and the pathogenesis of Kaposi's sarcoma. Annu Rev Pathol. 2006; 1:273–96. [PubMed: 18039116]

Gilbert JM, Benjamin TL. Early steps of polyomavirus entry into cells. J Virol. 2000; 74(18):8582–8. [PubMed: 10954560]

Giroglou T, Florin L, Schafer F, Streeck RE, Sapp M. Human papillomavirus infection requires cell surface heparan sulfate. J Virol. 2001; 75(3):1565–70. [PubMed: 11152531]

Graham KL, Fleming FE, Halasz P, Hewish MJ, Nagesha HS, Holmes IH, Takada Y, Coulson BS. Rotaviruses interact with alpha4beta7 and alpha4beta1 integrins by binding the same integrin domains as natural ligands. J Gen Virol. 2005; 86(Pt 12):3397–408. [PubMed: 16298987]

Greber UF. Signalling in viral entry. Cell Mol Life Sci. 2002; 59(4):608–26. [PubMed: 12022470]

Grundhoff A, Ganem D. Inefficient establishment of KSHV latency suggests an additional role for continued lytic replication in Kaposi sarcoma pathogenesis. J Clin Invest. 2004; 113(1):124–36. [PubMed: 14702116]

Hutt-Fletcher LM. Epstein-Barr virus entry. J Virol. 2007; 81(15):7825–32. [PubMed: 17459936]

Jarousse N, Chandran B, Coscoy L. Lack of heparan sulfate expression in B-cell lines: implications for Kaposi's sarcoma-associated herpesvirus and murine gammaherpesvirus 68 infections. J Virol. 2008; 82(24):12591–7. [PubMed: 18842731]

Kalia M, Jameel S. Virus entry paradigms. Amino Acids. 2009

Kock J, Borst EM, Schlicht HJ. Uptake of duck hepatitis B virus into hepatocytes occurs by endocytosis but does not require passage of the virus through an acidic intracellular compartment. J Virol. 1996; 70(9):5827–31. [PubMed: 8709200]

Krishnan HH, Naranatt PP, Smith MS, Zeng L, Bloomer C, Chandran B. Concurrent expression of latent and a limited number of lytic genes with immune modulation and antiapoptotic function by Kaposi's sarcoma-associated herpesvirus early during infection of primary endothelial and fibroblast cells and subsequent decline of lytic gene expression. J Virol. 2004; 78(7):3601–20. [PubMed: 15016882]

Krishnan HH, Sharma-Walia N, Zeng L, Gao SJ, Chandran B. Envelope glycoprotein gB of Kaposi's sarcoma-associated herpesvirus is essential for egress from infected cells. J Virol. 2005; 79(17): 10952–67. [PubMed: 16103147]

Lan K, Kuppers DA, Verma SC, Sharma N, Murakami M, Robertson ES. Induction of Kaposi's sarcoma-associated herpesvirus latency-associated nuclear antigen by the lytic transactivator RTA: a novel mechanism for establishment of latency. J Virol. 2005; 79(12):7453–65. [PubMed: 15919901]

Mackay RL, Consigli RA. Early events in polyoma virus infection: attachment, penetration, and nuclear entry. J Virol. 1976; 19(2):620–36. [PubMed: 183018]

Marsh M, Helenius A. Virus entry: open sesame. Cell. 2006; 124(4):729–40. [PubMed: 16497584]

Mercer J, Helenius A. Vaccinia virus uses macropinocytosis and apoptotic mimicry to enter host cells. Science. 2008; 320(5875):531–5. [PubMed: 18436786]

Mercer J, Helenius A. Virus entry by macropinocytosis. Nat Cell Biol. 2009; 11(5):510–20. [PubMed: 19404330]

Miller N, Hutt-Fletcher LM. Epstein-Barr virus enters B cells and epithelial cells by different routes. J Virol. 1992; 66(6):3409–14. [PubMed: 1316456]

Mocarski ES Jr. Propagating Kaposi's sarcoma-associated herpesvirus. N Engl J Med. 1997; 336(3): 214–5. [PubMed: 8988903]

Naranatt PP, Akula SM, Chandran B. Characterization of gamma2-human herpesvirus-8 glycoproteins gH and gL. Arch Virol. 2002; 147(7):1349–70. [PubMed: 12111412]

Naranatt PP, Akula SM, Zien CA, Krishnan HH, Chandran B. Kaposi's sarcoma-associated herpesvirus induces the phosphatidylinositol 3-kinase-PKC-zeta-MEK-ERK signaling pathway in target cells early during infection: implications for infectivity. J Virol. 2003; 77(2):1524–39. [PubMed: 12502866]

Naranatt PP, Krishnan HH, Smith MS, Chandran B. Kaposi's sarcoma-associated herpesvirus modulates microtubule dynamics via RhoA-GTP-diaphanous 2 signaling and utilizes the dynein motors to deliver its DNA to the nucleus. J Virol. 2005; 79(2):1191–206. [PubMed: 15613346]

Naranatt PP, Krishnan HH, Svojanovsky SR, Bloomer C, Mathur S, Chandran B. Host gene induction and transcriptional reprogramming in Kaposi's sarcoma-associated herpesvirus (KSHV/HHV-8)-infected endothelial, fibroblast, and B cells: insights into modulation events early during infection. Cancer Res. 2004; 64(1):72–84. [PubMed: 14729610]

Nicola AV, McEvoy AM, Straus SE. Roles for endocytosis and low pH in herpes simplex virus entry into HeLa and Chinese hamster ovary cells. J Virol. 2003; 77(9):5324–32. [PubMed: 12692234]

Nicola AV, Straus SE. Cellular and viral requirements for rapid endocytic entry of herpes simplex virus. J Virol. 2004; 78(14):7508–17. [PubMed: 15220424]

Pietiainen V, Marjomaki V, Upla P, Pelkmans L, Helenius A, Hyypia T. Echovirus 1 endocytosis into caveosomes requires lipid rafts, dynamin II, and signaling events. Mol Biol Cell. 2004; 15(11): 4911–25. [PubMed: 15356270]

Raghu H, Sharma-Walia N, Veettil MV, Sadagopan S, Caballero A, Sivakumar R, Varga L, Bottero V, Chandran B. Lipid rafts of primary endothelial cells are essential for Kaposi's sarcoma-associated herpesvirus/human herpesvirus 8-induced phosphatidylinositol 3-kinase and RhoA-GTPases critical for microtubule dynamics and nuclear delivery of viral DNA but dispensable for binding and entry. J Virol. 2007; 81(15):7941–59. [PubMed: 17507466]

Raghu H, Sharma-Walia N, Veettil MV, Sadagopan S, Chandran B. Kaposi's sarcoma-associated herpesvirus utilizes an actin polymerization-dependent macropinocytic pathway to enter human dermal microvascular endothelial and human umbilical vein endothelial cells. J Virol. 2009; 83(10):4895–911. [PubMed: 19279100]

Rappocciolo G, Hensler HR, Jais M, Reinhart TA, Pegu A, Jenkins FJ, Rinaldo CR. Human herpesvirus 8 infects and replicates in primary cultures of activated B lymphocytes through DC-SIGN. J Virol. 2008; 82(10):4793–806. [PubMed: 18337571]

Rappocciolo G, Jenkins FJ, Hensler HR, Piazza P, Jais M, Borowski L, Watkins SC, Rinaldo CR Jr. DC-SIGN is a receptor for human herpesvirus 8 on dendritic cells and macrophages. J Immunol. 2006; 176(3):1741–9. [PubMed: 16424204]

Sadagopan S, Sharma-Walia N, Veettil MV, Raghu H, Sivakumar R, Bottero V, Chandran B. Kaposi's sarcoma-associated herpesvirus induces sustained NF-kappaB activation during de novo infection of primary human dermal microvascular endothelial cells that is essential for viral gene expression. J Virol. 2007; 81(8):3949–68. [PubMed: 17287275]

Schulz TF, Sheldon J, Greensill J. Kaposi's sarcoma associated herpesvirus (KSHV) or human herpesvirus 8 (HHV8). Virus Res. 2002; 82(1-2):115–26. [PubMed: 11885938]

Sharma-Walia N, Krishnan HH, Naranatt PP, Zeng L, Smith MS, Chandran B. ERK1/2 and MEK1/2 induced by Kaposi's sarcoma-associated herpesvirus (human herpesvirus 8) early during infection of target cells are essential for expression of viral genes and for establishment of infection. J Virol. 2005; 79(16):10308–29. [PubMed: 16051824]

Sharma-Walia N, Naranatt PP, Krishnan HH, Zeng L, Chandran B. Kaposi's sarcoma-associated herpesvirus/human herpesvirus 8 envelope glycoprotein gB induces the integrin-dependent focal adhesion kinase-Src-phosphatidylinositol 3-kinase-rho GTPase signal pathways and cytoskeletal rearrangements. J Virol. 2004; 78(8):4207–23. [PubMed: 15047836]

Sieczkarski SB, Whittaker GR. Dissecting virus entry via endocytosis. J Gen Virol. 2002; 83(Pt 7): 1535–45. [PubMed: 12075072]

Sinzger C. Entry route of HCMV into endothelial cells. J Clin Virol. 2008; 41(3):174–9. [PubMed: 18203656]

Stang E, Kartenbeck J, Parton RG. Major histocompatibility complex class I molecules mediate association of SV40 with caveolae. Mol Biol Cell. 1997; 8(1):47–57. [PubMed: 9017594]

Staskus KA, Zhong W, Gebhard K, Herndier B, Wang H, Renne R, Beneke J, Pudney J, Anderson DJ, Ganem D, Haase AT. Kaposi's sarcoma-associated herpesvirus gene expression in endothelial (spindle) tumor cells. J Virol. 1997; 71(1):715–9. [PubMed: 8985403]

Stewart PL, Nemerow GR. Cell integrins: commonly used receptors for diverse viral pathogens. Trends Microbiol. 2007; 15(11):500–7. [PubMed: 17988871]

Triantafilou K, Takada Y, Triantafilou M. Mechanisms of integrin-mediated virus attachment and internalization process. Crit Rev Immunol. 2001; 21(4):311–22. [PubMed: 11922076]

Tufaro F. Virus entry: two receptors are better than one. Trends Microbiol. 1997; 5(7):257–8. discussion 258-9. [PubMed: 9234500]

Tyagi M, Rusnati M, Presta M, Giacca M. Internalization of HIV-1 tat requires cell surface heparan sulfate proteoglycans. J Biol Chem. 2001; 276(5):3254–61. [PubMed: 11024024]

Veettil MV, Sadagopan S, Sharma-Walia N, Wang FZ, Raghu H, Varga L, Chandran B. Kaposi's sarcoma-associated herpesvirus forms a multimolecular complex of integrins (alphaVbeta5, alphaVbeta3, and alpha3beta1) and CD98-xCT during infection of human dermal microvascular endothelial cells, and CD98-xCT is essential for the postentry stage of infection. J Virol. 2008; 82(24):12126–44. [PubMed: 18829766]

Veettil MV, Sharma-Walia N, Sadagopan S, Raghu H, Sivakumar R, Naranatt PP, Chandran B. RhoA-GTPase facilitates entry of Kaposi's sarcoma-associated herpesvirus into adherent target cells in a Src-dependent manner. J Virol. 2006; 80(23):11432–46. [PubMed: 17005646]

Verma SC, Lan K, Robertson E. Structure and function of latency-associated nuclear antigen. Curr Top Microbiol Immunol. 2007; 312:101–36. [PubMed: 17089795]

Wang FZ, Akula SM, Pramod NP, Zeng L, Chandran B. Human herpesvirus 8 envelope glycoprotein K8.1A interaction with the target cells involves heparan sulfate. J Virol. 2001; 75(16):7517–27. [PubMed: 11462024]

West J, Damania B. Upregulation of the TLR3 pathway by Kaposi's sarcoma-associated herpesvirus during primary infection. J Virol. 2008; 82(11):5440–9. [PubMed: 18367536]

WuDunn D, Spear PG. Initial interaction of herpes simplex virus with cells is binding to heparan sulfate. J Virol. 1989; 63(1):52–8. [PubMed: 2535752]

Zhong W, Wang H, Herndier B, Ganem D. Restricted expression of Kaposi sarcoma-associated herpesvirus (human herpesvirus 8) genes in Kaposi sarcoma. Proc Natl Acad Sci U S A. 1996; 93(13):6641–6. [PubMed: 8692871]

Zhu L, Puri V, Chandran B. Characterization of human herpesvirus-8 K8.1A/B glycoproteins by monoclonal antibodies. Virology. 1999; 262(1):237–49. [PubMed: 10489357]

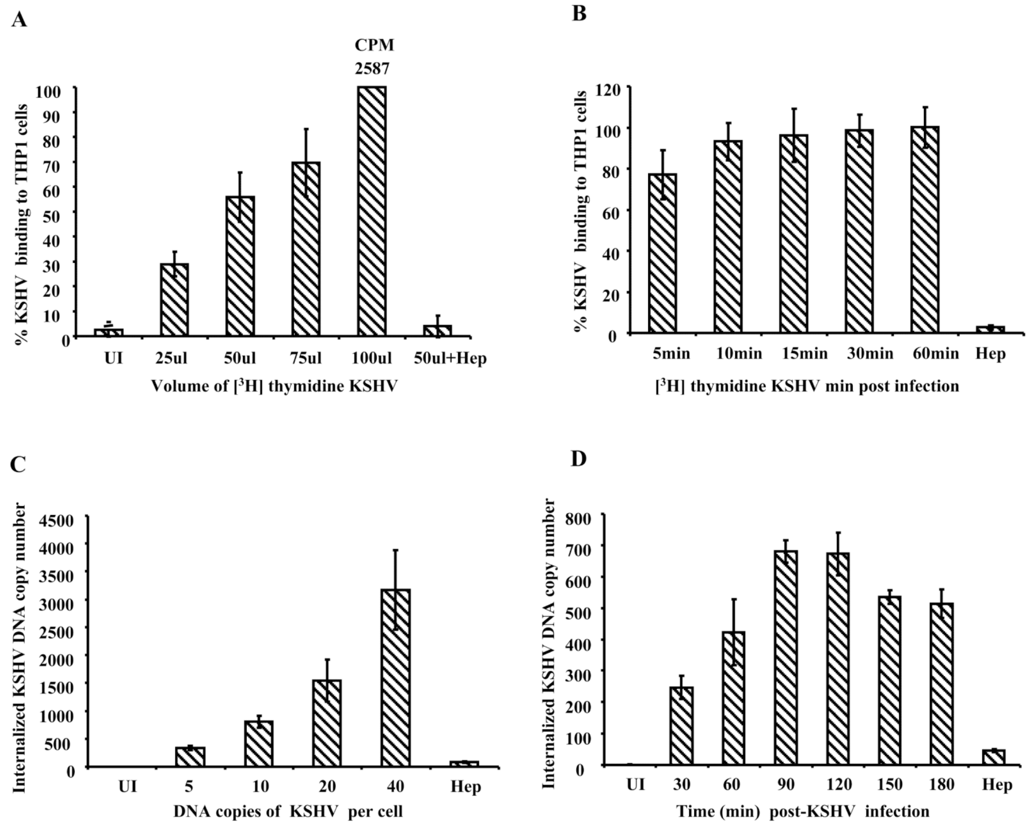

Figure 1.

A and B: KSHV binding assays. 1×10^6 THP-1 cells left uninfected (UI) or were incubated with an increasing amount of [^{3}H] thymidine labeled purified KSHV for 1 h at 4°C **(A)** or with 50μl of labeled KSHV for indicated time points **(B)**. The cells were washed, lysed, and precipitated with trichloroacetic acid, and the cell-associated virus counts per minute (cpm) were determined. Each reaction was done in duplicate, and each point represents the average ± SD of three experiments. As specificity control, [^{3}H] thymidine labeled KSHV were pretreated with heparin (100μg/ml) for 1 h and then incubated with the target cells for 1 h at 4°C. **C and D: KSHV entry into THP-1 cells (C)** 0.5×10^6 THP-1 cells were incubated with different DNA copies per cell. Two hours p.i., unbound and uninternalized viruses were removed by washing and trypsinization. **(D)** 1×10^6 THP-1 cells were infected with 10 KSHV DNA copies per cell and at different time points and uninternalized viruses removed by washing and trypsinization. For C and D, internalized viral copy numbers were determined by real-time DNA PCR with taqman probe and primers specific for ORF73. Viral DNA copy numbers were calculated based on the standard curve generated by using known concentrations of the cloned ORF73 gene. Percent internalization of KSHV was calculated by considering maximum internalized virus DNA copy number as 100%. Each time point represents the average ± SD of three experiments.

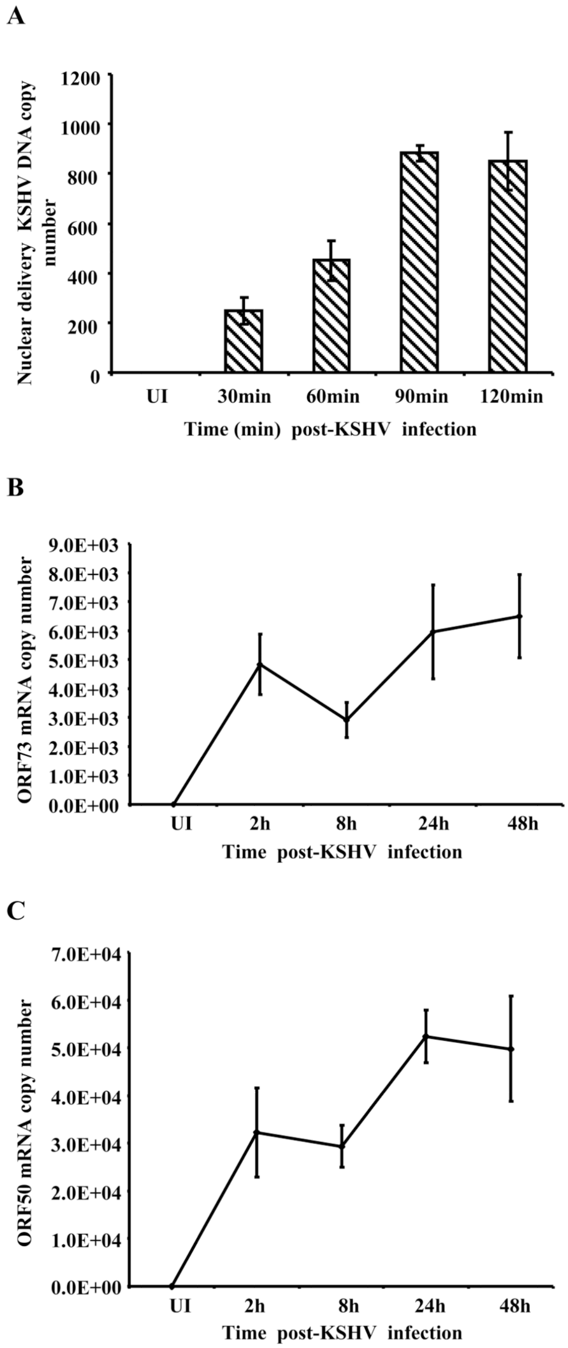

Figure 2.

A. Kinetics of KSHV genome delivery into infected cell nuclei. 1×10^6 THP-1 cells were infected with 10 KSHV DNA copies per cell. At different time points, uninternalized virus was removed by washing and trypsinization. Nuclei were isolated and purity of the isolated nuclei was determined by the presence of lamin B and absence of tubulin in western blotts of the isolated nuclei. 100ng of DNA purified from infected cell nuclei was used to determine the number of KSHV DNA copies delivered to nuclei by real-time DNA PCR for the ORF73 gene as described in the figure 1C and D legend. **B and C. Kinetics of KSHV gene expression in THP-1 cells**. 1×10^6 THP-1 cells were infected with 30 KSHV DNA copies per cell. At different time points p.i., RNA was isolated, treated with DNase I, and

250 ng of DNase-treated RNA was subjected to real-time RT-PCR with primers and Taqman probes for the ORF 73 and 50 genes. Known concentrations of DNase-treated in vitro-transcribed ORF 50 and ORF 73 transcripts were used to construct a real-time RT-PCR standard curve from which the relative copy numbers of viral transcripts were determined and normalized to 18s rRNA used as internal control.

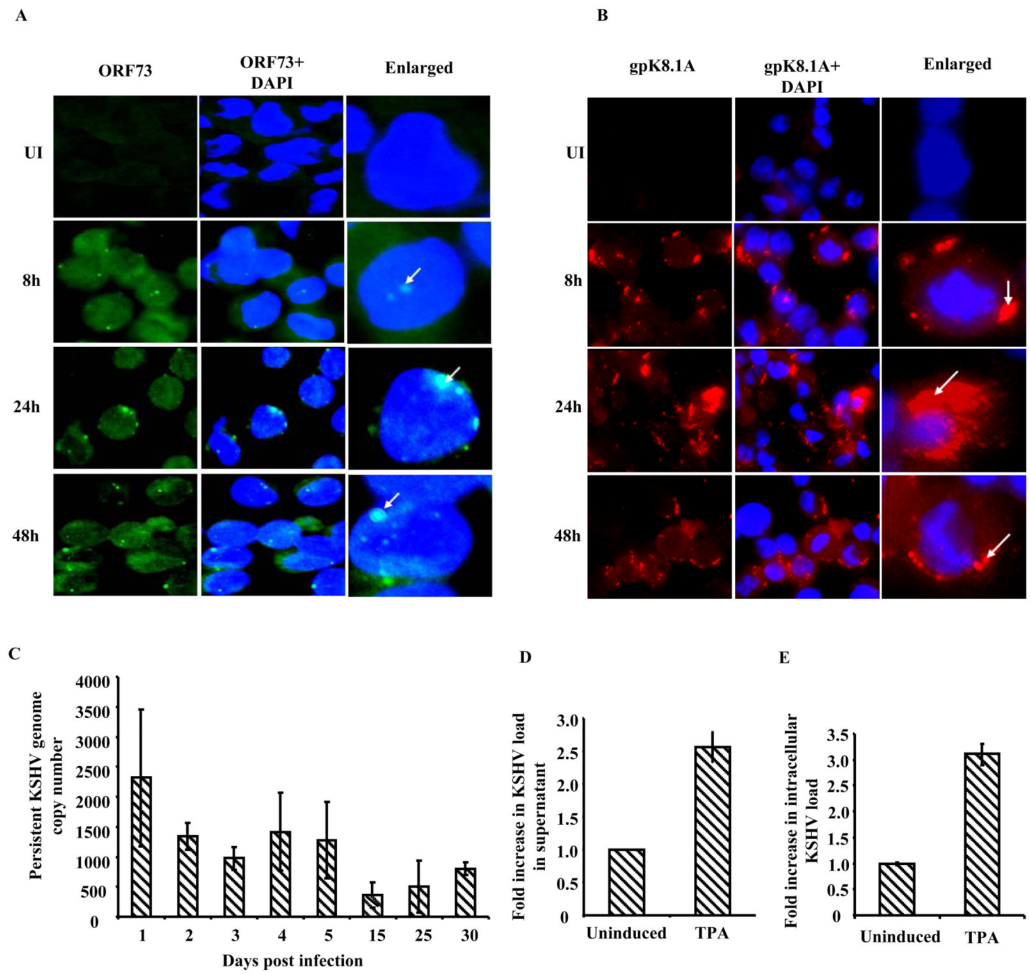

Figure 3.

A and B: Immunofluorescence analysis of LANA-1 and gpK8.1A expression. THP-1 cells were infected with 30 KSHV DNA copies per cell for 2 h and uninternalized viruses were removed by washing and trypsinization. Infected and uninfected cells were further incubated at 37°C, washed, fixed in 2 % paraformaldehyde for 10 min, permeabilized with 0.2% Triton X-100 for 5 min and blocked with Image-iT™ FX signal enhancer. Cells were stained with LANA and gpK8.1A antibodies and visualized by fluorescence microscopy. LANA-1 **(A)** and gpK8.1A **(B)** were visualized by incubation with Alexa-488 (green) and Alexa 594 (red) secondary antibodies, respectively, and cell nuclei were visualized by staining with DAPI (blue). The white arrows point at the expression of LANA-1 and gpK8.1A in infected cells. **C. Detection of persistent KSHV infection**. $1{\times}10^6$ THP-1 cells infected with KSHV (10 DNA copies per cell) for 2 h p.i., were washed, trypsinized and incubated for 1, 2, 3, 4, 5, 15, 25 and 30 days in complete medium. KSHV copy number persisting in THP-1 cells was determined by real-time DNA PCR for ORF73 as per legend in Figure 1 C and D. Each bar represents the number of KSHV genomes per $1{\times}10^6$ THP-1 cells; the values were derived upon normalizing with total DNA from each sample. **D and E. KSHV lytic reactivation in infected THP1 cells**. THP1 cells infected with KSHV for 2h, uninternalized viruses removed by washing and trypsinization and infected cells were cultured for 21 days in complete media. At 21 days p.i. these cells were either left untreated or treated with TPA (20ng/ml) for 5 days. KSHV lytic reactivation was assessed in cell culture supernatant (D) and in cells (E) by determining the viral genome copy number by real-time DNA PCR as per legend in Figure 1 C and D. The values represent the fold increase in KSHV genome copy number in TPA treated cells compared untreated cells.

NIH-PA Author Manuscript
NIH-PA Author Manuscript

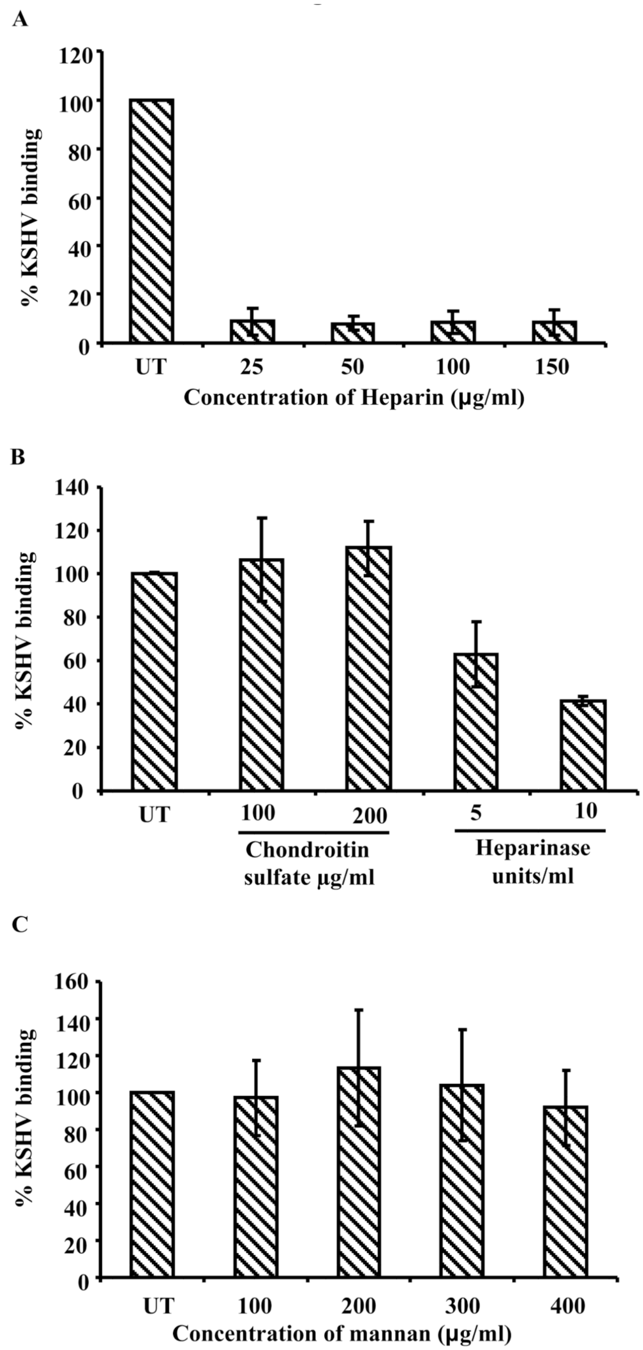

Figure 4.

A. KSHV binding in the presence of heparin. 1×10^6 THP-1 cells were incubated with heparin (25µg to 150µg/ml) pretreated [^{3}H] thymidine labeled KSHV or untreated labeled KSHV at 4° C for 1 h. The cell-associated virus was quantified as described under the figure 1 A and B legend. Each reaction was done in duplicate, and each point represents the average ± SD of three experiments. The cell bound virus in the presence of heparin was expressed as the percentage of virus binding compared to that of untreated THP-1 cells. **B KSHV binding in presence of chondroitin sulfate and in heparinase treated THP1 cells**. Chondroitin sulfate pretreated or untreated KSHV were incubated with 1×10^6 THP-1 cells (fixed with 0.1% paraformaldehyde) at 4° C for 1 h or heparinase I and III treated (5 and 10 units/ml, for 2 h at 37° C) THP1 cells were mildly fixed with 0.1% paraformaldehyde and incubated with KSHV 4° C for 1 h. The unbound viruses were removed by washing. The cell-bound virus was quantified by real-time DNA PCR as described in the 1 C and D legend. Each point represents the average ± SD of three experiments. The cell bound virus in the presence of chondroitin sulfate or in the heparinase treated THP1 was expressed as the percentage of virus binding compared to that of untreated controls. **C. KSHV binding in the presence of mannan**. $1{\times}10^6$ THP-1 cells mock treated or pre-incubated with the indicated concentrations of mannan at 4° C for 1 h. The cell-associated virus was quantified as described under the figure 1 A and B legend. Each reaction was done in duplicate, and each point represents the average ± SD of three experiments. The cell bound virus in the presence of mannan was expressed as the percentage of virus binding compared to that of untreated THP-1 cells.

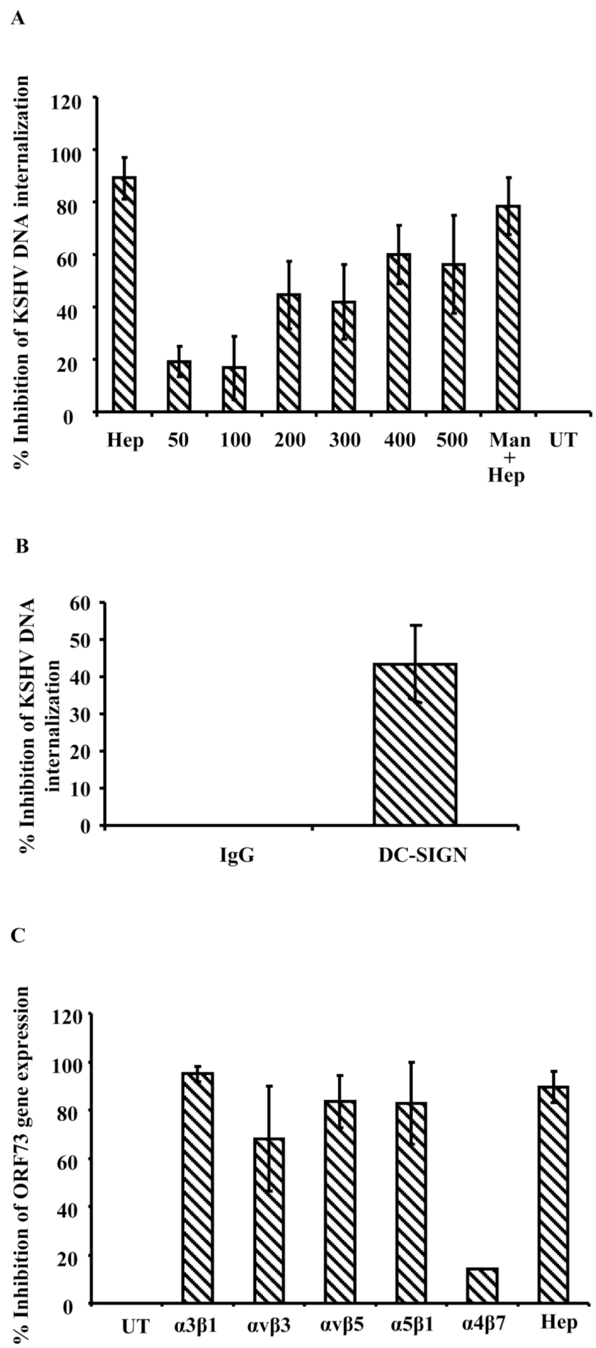

Figure 5.

A. KSHV internalization in the presence of heparin and mannan. 1×10^6 THP-1 cells mock treated or pre-incubated with the indicated concentrations of mannan at 4°C were infected with 10 KSHV DNA copies per cell or heparin pretreated KSHV (100ug/ml). At different time points, uninternalized virus was removed by washing and trypsinization. Infected and mock infected cells were washed and internalized viral copy numbers were determined by real-time DNA PCR as described in the figure 1C/D legend. The data are represented as the percent inhibition of KSHV DNA internalized in comparison with cells incubated with virus alone. Each reaction was done in duplicate and each bar represents the mean ± SD of the results of three experiments. **B. KSHV internalization in THP1 cells**

upon blocking DC-SIGN. THP1 cells incubated with mouse IgG or mouse anti-DC-SIGN mAb at 4° C for 1 h. The washed cells were incubated with KSHV (10 genome copies/cell) at 4° C for 1 h followed by at 37° C for 1 h. Uninternalized virus was removed by washing and trypsinization, internalized viral copy numbers were determined by real-time DNA PCR as described in the figure 1C/D legend. The data are represented as the percent inhibition of KSHV DNA internalization in comparison with IgG control. **C. KSHV gene expression in the presence of soluble integrins**. 1×10^6 THP-1 cells were infected with 30 KSHV DNA copies per cell of untreated virus or with virus pretreated with 10μg/ml of soluble α3β1, αvβ3, αvβ5, α5β1 and α4β7 integrins for 1 h at 37° C. At 2 h p.i. uninternalized virus was removed by washing and trypsinization and the infected cells were further incubated. At 24 h p.i., the cells were washed, RNA was isolated, ORF73 gene expression was examined as described under the figure 2B legend. ORF73 gene expression was represented as percent inhibition compared to control untreated KSHV infection.

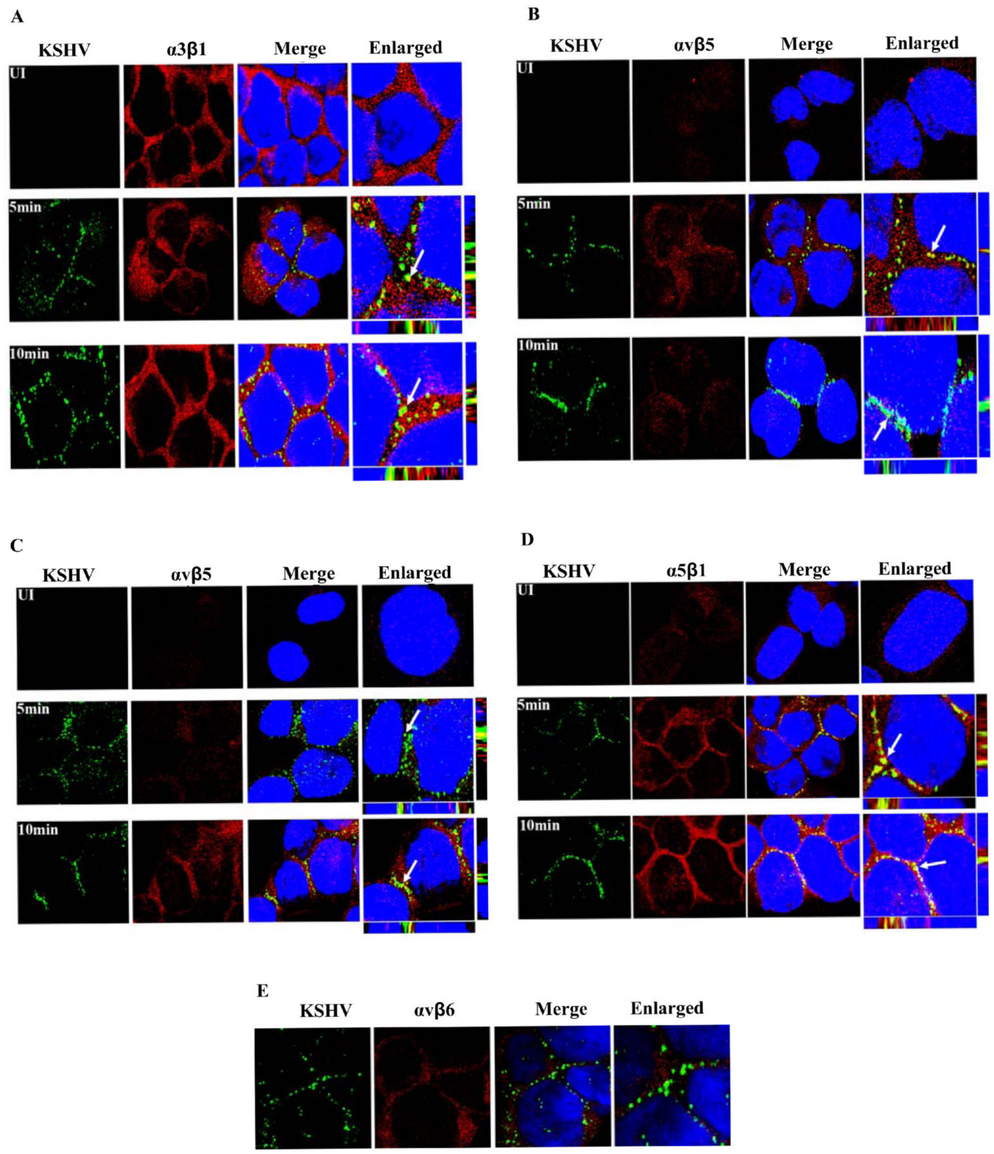

Figure 6. Immunofluorescence analysis of KSHV association with integrins

THP-1 cells were infected with 10 KSHV DNA copies per cell for 5 and 10 min. The cells were fixed in 2 % paraformaldehyde for 10 min, permeabilized with 0.2% Triton X-100 for 5 min and blocked. Infected and uninfected cells were stained with anti-KSHV gB and anti-α3β1/αvβ3/αvβ5/α5β1/αvβ6 integrin antibodies and visualized by confocal microscopy. KSHV-gB and integrins were visualized by incubation with Alexa-488 secondary antibody (green) and Alexa-594 secondary antibody (red), respectively. The arrows indicate the areas of KSHV co-localization with integrins. **A**. KSHV+ α3β1; **B**. KSHV+ αvβ3; **C**. KSHV+ αvβ5; **D**. KSHV+ α5β1; **E**. KSHV+ αvβ6.

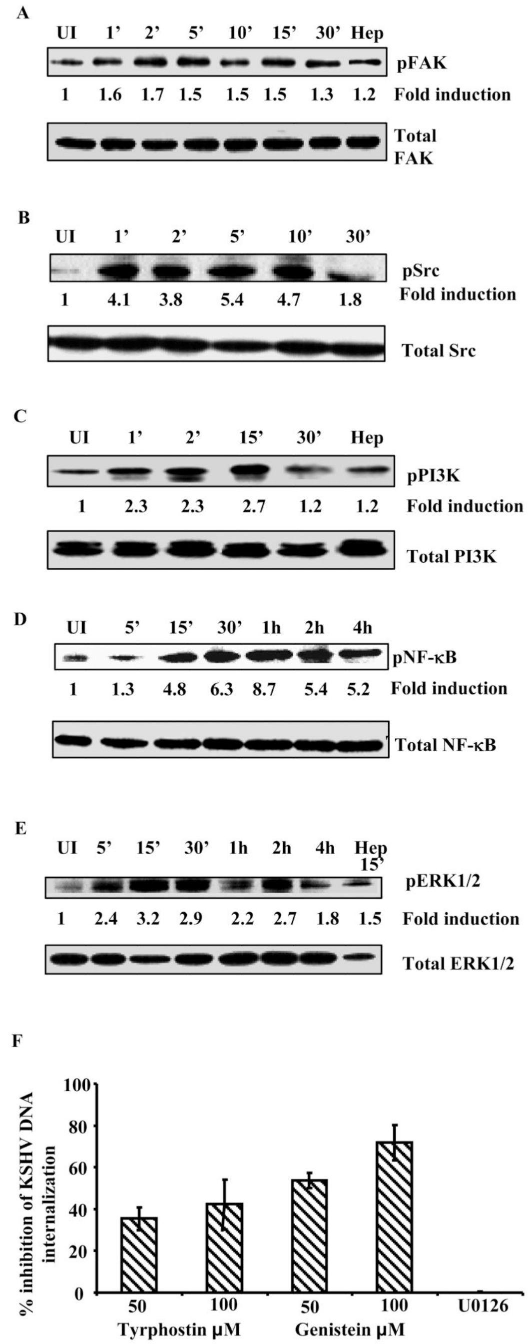

Figure 7. Signal induction during KSHV de novo infection of THP-1 cells

THP-1 cells, serum starved for 24 h, were left uninfected or infected with KSHV (20 DNA copies/cell) for the indicated time. Proteins prepared (15μg) from the infected and uninfected THP-1 were resolved by SDS-PAGE and transferred onto nitrocellulose membranes. Phosphorylated and total **(A)** FAK, **(B)** Src, **(C)** PI3K, **(D)** NF-κB and **(E)** ERK1/2 proteins were detected with the respective antibodies. The fold induction of phosphorylation was calculated based on the ratio of phosphorylated/total at each time point and values represent fold phosphorylation compared uninfected. HS pretreated KSHV (1 h at 37°C) was used as control. **(F) Effect of tyrphostin and genistein on KSHV internalization**. Untreated and THP-1 cells preincubated with Tyrphostin and Genistein (1 h at 37° C) were infected with KSHV. At 2 h p.i., mock treated and treated cells were washed and trypsinized to remove uninternalized viruses. Internalized KSHV copy number was determined as described in figure legend 1C/D. The data are represented as the percent inhibition of KSHV DNA internalization in comparison with untreated THP-1 cells.

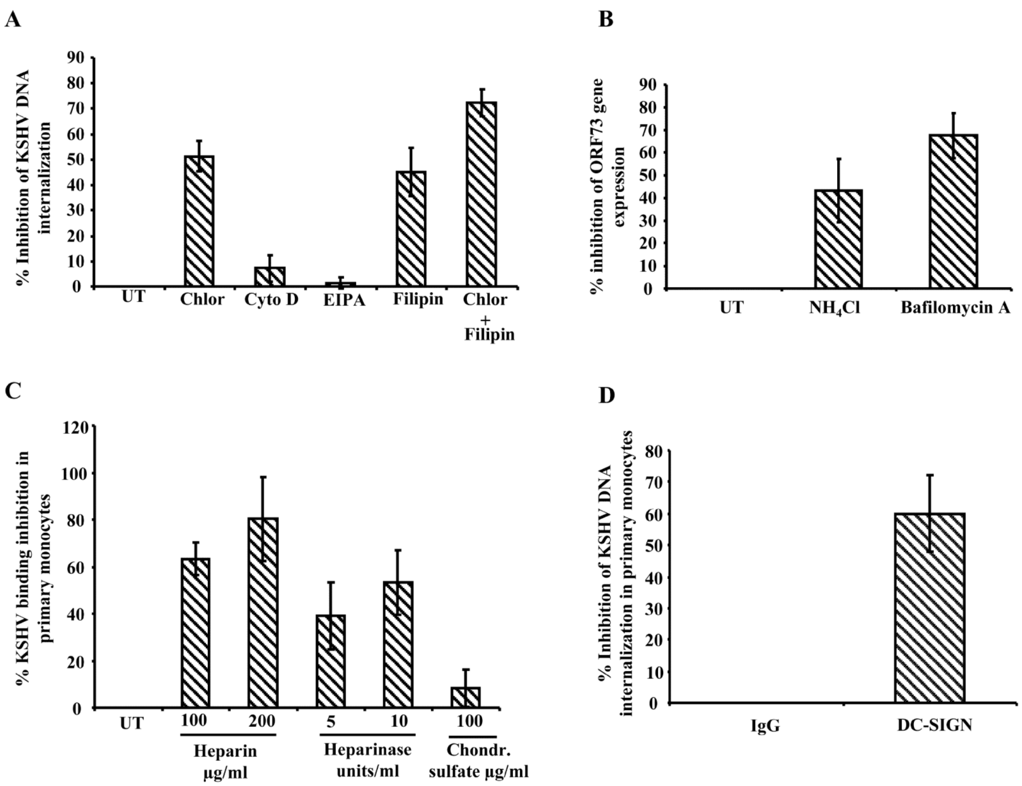

Figure 8.

A. Effect of endocytosis inhibitors on KSHV infection of THP-1 cells. Mock treated and THP-1 cells pre-incubated with chlorpromazine (Chlor), cytochelasin D (Cyto D), EIPA and filipin (1 h at 37° C) were infected with KSHV. At 2 h p.i., untreated (UT) and treated cells were washed and trypsinized to remove uninternalized viruses and then internalized KSHV copy number was determined as described in figure legend 1C/D. The data are represented as the percent inhibition of KSHV DNA internalization in comparison with untreated THP-1 cells. **B. Effect of endosomal acidification inhibitor on KSHV infection of THP-1 cells**. THP-1 cells either left untreated (UT) or preincubated with NH_4Cl (100mM) for 3 h and bafilomycin (50nM) for 1 h, incubated with KSHV for 2 h and untreated and treated THP-1 cells were washed to remove uninternalized virus. Cells were incubated in complete medium for 24 h, RNA was isolated and ORF73 expression was examined as described in figure legend 2B. The data are represented as the percent inhibition of KSHV ORF73 gene expression in comparison with untreated THP-1 cells. **C. Role of heparan sulfate and chondroitin sulfate in KSHV binding in primary monocytes**. Chondroitin sulfate/heparin pretreated or untreated KSHV were incubated with 1×10^5 primary monocytes (fixed with 0.1% paraformaldehyde) at 4° C for 1 h or heparinase I and III treated (5 and 10 units/ml, for 2 h at 37° C) primary monocytes were mildly fixed with 0.1% paraformaldehyde and incubated with KSHV 4° C for 1 h. The unbound viruses were removed by washing. The cell-bound virus was quantified by realtime DNA PCR as described in the 1 C and D legend. Each point represents the average ± SD of three experiments. The cell bound virus in the presence of chondroitin sulfate/heparin or in the heparinase treated cells was expressed as the percentage of virus binding compared to that of untreated controls. **D. KSHV internalization in primary monocytes upon blocking DC-SIGN**. Primary monocytes incubated with mouse IgG or mouse anti-DC-SIGN mAb at 4° C for 1 h. The washed cells were incubated with KSHV (10 genome copies/cell) at 4° C for 1 h followed by at 37° C for 1 h. Uninternalized virus was removed by washing and trypsinization, internalized viral copy numbers were determined by real-time DNA PCR as described in the figure 1C/D legend. The data are represented as the percent inhibition of KSHV DNA internalization in comparison with IgG control.

NIH-PA Author Manuscript
NIH-PA Author Manuscript